Desalination and Water Treatment
www.deswater.com
doi: 10.5004/dwt.2020.26190

203 (2020) 327–355
November

The efficient removal of the hazardous azo dye Acid Orange 7 from water using modified biochar from Pea-peels

Mohamed A. El-Nemr[a], Nabil M. Abdelmonem[a], Ibrahim M.A. Ismail[a,b], Safaa Ragab[c], Ahmed El Nemr[c,*]

[a]*Department of Chemical Engineering, Faculty of Engineering, Cairo University, Giza, Egypt, emails: mohamedelnemr1992@yahoo.com (M.A. El-Nemr), nabil_abdelmonem@yahoo.com (N.M. Abdelmonem), ibrahim.ismail@zewailcity.edu.eg (I.M.A. Ismail)*
[b]*Renewable Energy Program, Zewail City of Science and Technology, Egypt*
[c]*Environmental Division, National Institute of Oceanography and Fisheries, Kayet Bey, El-Anfoushy, Alexandria, Egypt, emails: ahmedmoustafaelnemr@yahoo.com/ahmed.m.elnemr@gmail.com (A. El Nemr), safaa_ragab65@yahoo.com (S. Ragab)*

Received 13 March 2020; Accepted 29 May 2020

ABSTRACT

In this study, we developed modified biochars and assessed its use for enhancing the adsorption capacity of Acid Orange 7 (AO7) dye. The removal of AO7 dye using unmodified (Pea-B) and modified (Pea-BO-NH_2 and Pea-BO-TETA) biochars derived from the pea *Pisum sativum* peels were investigated at room temperature using batch adsorption method. The adsorption behavior of biochars toward AO7 dye was studied using different parameters such as dye concentrations, biochar dosage, contact time, and pH. The results reveal that the optimum conditions for the maximum adsorption of AO7 dye are at pH 2 and contact time 3 h. The adsorption capacity at equilibrium (q_e) of the modified biochar was significantly enhanced from 78.18 to 523.12 mg g^{-1}. Pea-BO-TETA biochar had the largest adsorption capacity (523.12 mg g^{-1}) at initial concentration 300 mg L^{-1} and dosage 0.50 g L^{-1}. The percentage removal of AO7 dye reached 99% for Pea-BO-NH_2, 98% for Pea-BO-TETA, and 96% for Pea-B biochars. The structure of the prepared Pea-peel biochars was characterized by Brunauer–Emmett–Teller and Barrett–Joyner–Halenda methods, scanning electron microscopy, Fourier-transform infrared spectroscopy (FTIR), thermogravimetric analysis and energy-dispersive X-ray spectroscopy (EDAX) analyses. The enhanced of AO7 dye adsorption by modified biochars could be attributed to the increasing surface NH_2 group content which was confirmed by FTIR spectra and EDAX analysis. The results obtained from batch experiments were analyzed by various isotherm models and the error function equations were applied to find the best-fit isotherm model. Freundlich model reported the best fit for the experimental data. The experiment data was primarily obeyed by pseudo-second-order rather than the other studied kinetic models.

Keywords: Pea-peels; *Pisum sativum*; Biochar; Adsorption; Acid Orange 7 dye; Water treatment

1. Introduction

Today, the pollution and the scarcity of freshwater have become pressing issues and required urgent worldwide concern. Therefore, the treatment and reutilization of water are becoming essential for facing water stress problems in the world. Wastewater effluents of highly charged with pollutants produced from dyeing, printing, and textile industries are representing a serious threat to the environment [1,2]. Among these pollutes, organic dyes are considered as the most toxic, carcinogenic, and mutagenic compounds even at low concentrations [3,4]. Recently many industries were

* Corresponding author.

used synthetic organic dyes in their production, such as textiles, pharmaceuticals, plastics, printing, paper, food, leather, and cosmetics [5,6]. The textile industry is responsible for 15% to 20% of worldwide water pollution [7,8]. Nowadays, globally there were about 10,000 different dyes are produced and the annual global dyes production is approximated at 7.105 tons [9,10]. Almost 10% of these dyes are rejected directly in the natural environment without treatment to reduce their polluting components to the surrounding environment, and these liquid wastes cause serious health problems for humans such as skin irritation, eye irritation, mucous membranes irritation and irritation of the upper respiratory tract, as well as nausea and headache. Diseases caused by this polluted water include skin infections and anemia as a result of bone marrow loss [11,12].

Most azo dyes are tending to be quite persistent in the environment and resistant to biodegradation due to the presence of one or more azo bonds (–N=N–), a large number of aromatic groups, and auxochromes (e.g., $–SO_3$ and –OH) [13]. Plenty of attempts for the treatment of organic azo dyes from industrial effluents have been extensively developed to mitigate their threat to the environment [14]. However, conventional methods such as coagulation, precipitation, photocatalytic degradation, ozonation, desalination, etc. for the treatment of dye-containing wastewater are found to be limited and ineffective [15–23]. The adsorption method has been currently widely used to be of better quality to other wastewater handling methods because it is owing to many advantages such as low cost, simple design, easy handling property, high efficiency, and less susceptibility to poisonous substances [24]. Biochar can be used with a range of applications such as an agent for soil improvement, an avenue for greenhouse gas mitigation, and remediation of the particular environmental pollution. Biochar can be used as an efficient adsorbent for the removal of many pollutants such as dyes [25,26], chromium [27], heavy metals [28], and pentachlorophenol [29]. Amberlite Ira-938 resin was used to adsorb of rose bengal dye from aqueous solution [30], arginine modified activated carbon was tested for removing of cationic dye from aqueous medium [31], and degradation of congo-red dye using gamma radiation was reported [32].

It is worth mentioning that there is a relationship between feedstock structure, processing conditions, and physical characteristics of biochar. Density, surface area, micro- and macro pores formation, particle size, and pore size distribution are important biochar physical characteristics. The most commonly observed feature in processed biochar is a pore structure. To enhance the removal efficiency and adsorption capacity of biochar, the modification can take place by loading biochar before, during, or after preparation with reluctant, minerals, functional groups, nanoparticles, and activation with basic solution [33]. However, the original adsorption capacity of unmodified biochar is low and enhancement is thus urgently required. Modernity in this work is the use of Pea-peels in the preparation of biochar for the first time and then treating biochar produced with ozone followed by ammonium hydroxide to form amine groups on the surface of biochar to increase its ability to absorb dyes from water. The high nitrogen content introduced into the new biochar prepared from Pea-peels as a worthless waste has resulted in the production of new good quality materials that have a great ability to absorb dyes from water.

The present study was aimed at producing novel modified biochars (Pea-BO-NH_2 and Pea-BO-TETA) adsorbent from Pea-peels and using them to remove the Acid Orange 7 (AO7) dye from water. The characteristics of the modified biochars were analyzed by Fourier-transform infrared spectroscopy (FTIR), scanning electron microscopy (SEM), energy-dispersive X-ray spectroscopy (EDAX), Brunauer–Emmett–Teller (BET) and Barrett–Joyner–Halenda (BJH) analyses. The thermal stability was examined by thermogravimetric analysis (TGA), differential thermal analysis (DTA), and differential scanning calorimetry (DSC) analyses. The adsorption properties of the obtained biochars to AO7 dye, including the adsorption kinetics and the isothermal properties, were also investigated.

2. Materials and methods

2.1. Materials

Pea-peels raw material was collected from a local market for the preparation of biochar. Acid Orange 7 (Orange II) (C.I. 15510) ($C_{16}H_{11}N_2NaO_4S$) (Mwt = 350) was purchased from Sigma-Aldrich (USA). Sulphuric acid (H_2SO_4, M.W. = 98.07 g, assay (acid-metric) 99%), ammonia solution (NH_4OH, M.W. = 35 g, assay 25%) and triethylenetetramine (TETA) were purchased from Sigma-Aldrich (USA).

2.2. Preparation of biochars

2.2.1. Preparation of Pea-peel biochar (Pea-B)

Pea-peels were thoroughly washed with tap water to remove dust and the cleaned Pea-peels were dried in an oven at 105°C for 48 h, and the dried Pea-peels were milled and crushed. The crushed Pea-peels (25.0 g) was boiled in a 100 mL solution of 50% H_2SO_4 in a refluxed system for 2 h, then the reaction mixture was filtered and washed with distilled water until the filtrate become neutral followed by washing with ethanol. The final product of biochar was dried in the oven at 70°C overnight, and then its weight is determined. The obtained biochar from this reaction was labeled as Pea-B biochar. In this preparation method, the carbonization and sulphonation processes occurred.

2.2.2. Chemical surface modification of Pea-B biochar

Dried Pea-B biochar was subjected to a two stages modification. At the first stage, the Pea-B biochar which prepared as mentioned above was ozonized in water for 2 h. Then the ozone activated biochar was allowed to dry in an oven at 70°C overnight after washing with distilled water and ethanol and the product was labeled as Pea-BO biochar. This stage is urgent to increase the surface oxygen content for increasing its ability for grafting with amine functional groups.

In the second stage, two amine-functionalized biochars were prepared by grafting with ammonium hydroxide (NH_4OH) and TETA. For functionalized Pea-BO biochar with NH_4OH, the Pea-BO biochar (25 g) was boiled in a 100 mL solution of 25% NH_4OH in a refluxed system for 2 h, followed

by filtration, then washed with distilled water and ethanol. The final product of biochar was dried in the oven at 70°C overnight, and then its weight is determined (~32.50 g yield). The product was labeled as Pea-BO-NH_2 biochar. For functionalized Pea-BO biochar with TETA, the biochar Pea-BO (25 g) was boiled in 100 mL solution of TETA in a refluxed system for 2 h, then the reaction mixture was filtered and washed with distilled water and ethanol. The final product was dried at 70°C overnight, then its weight is determined (~36.2 g yield). The product was labeled as Pea-BO-TETA biochar.

2.3. Batch adsorption experimental

A stock solution containing 1,000 mg L^{-1} of Acid Orange 7 dye prepared by dissolving 1.0 g of AO7 dye in 1,000 mL of double-distilled water. The adsorption experiments were carried out by the batch equilibrium method. 100 mL of the adsorbate solution was agitated with different doses of the prepared adsorbent in a shaker (JSOS-500, Korea). The solution was analyzed for the residual AO7 dye concentration using a visible-UV spectrophotometer at adsorption wavelength of λ_{max} 483 nm. The adsorption capacities (q_t, mg g^{-1}) of the adsorbent at time t were calculated using Eq. (1).

$$q_t = \frac{\left(C_0 - C_t\right)}{W} \times V \tag{1}$$

where the initial concentration of dye is C_0 (mg L^{-1}); the residual concentration of the dye at time t is C_t (mg L^{-1}); V (L) is the volume of dye solution and W (g) is mass of biochar in gram. The removal percentage of AO7 dye from aqueous solution is computed using the following equation.

$$\text{Removal}\left(\%\right) = \frac{\left(C_0 - C_t\right)}{C_0} \times 100 \tag{2}$$

The effect of pH on AO7 dye removal was studied by adding 0.5 g of the adsorbent to 100 mL of 100 mg L^{-1} of AO7 dye solution for pea biochar with initial pH values 2, 4, 5.5, 7, and 9. The pH values were adjusted with 0.1 M HCl and NaOH solutions. The reaction mixture was shaken at 200 rpm for 15, 30, 45, 60, 90, 120, and 180 min at room temperature and sampled for AO7 dye color analysis.

The isotherm study was performed using various concentrations of AO7 dye solutions 75, 100, 150, and 200 mg L^{-1} for Pea-B, 100, 150, 200, and 300 mg L^{-1} for Pea-BO-NH_2 and Pea-BO-TETA biochars. Mixtures of 0.2, 0.3, 0.4, 0.5, and 0.6 g of the Pea-B, mixtures of 0.05, 0.1, 0.125, 0.15, and 0.2 g of the Pea-BO-NH_2 and Pea-BO-NH_2 with 100 mL AO7 dye solutions of various initial concentrations were shaken at 200 rpm for 180 min at 25°C.

The effect of biochar dose and contact time on AO7 dye adsorption was studied by shaking 100 mL of 75, 100, 150, and 200 mg L^{-1} of initial dye concentration for Pea-B and 100, 150, 200, and 300 mg L^{-1} for Pea-BO-NH_4OH and Pea-BO-TETA biochars with Pea-B different adsorbent doses of 0.2, 0.3, 0.4, 0.5, and 0.6 g and Pea-BO-NH_4OH and Pea-BO-TETA doses of 0.05, 0.1, 0.125, 0.15, and 0.2 g at different interval times of 0, 15, 30, 45, 60, 90, 120, and 180 min at 25°C.

2.4. Characterization

2.4.1. Nitrogen adsorption measurements

The adsorption–desorption isotherm of nitrogen gas on biochar was determined at the boiling point of N_2 gas. The BET surface area (S_{BET}) measurements of the biochar were made by nitrogen adsorption at 77 K using surface area and pore analyzer (BELSORP – Mini II, BEL Japan, Inc., Japan) [34,35]. Analysis of the isotherm was carried out by applying the BET plot to obtain monolayer volume (V_m) (cm^3 (STP) g^{-1}), the surface area (S_{BET}) (m^2 g^{-1}), total pore volume (p/p_0) (cm^3 g^{-1}), (C) energy constant and mean pore diameter (nm). The average pore radius was calculated by using the following Eq. (3).

$$r\left(\text{nm}\right) = \frac{2V_T\left(\text{mL g}^{-1}\right)}{a_{s,\text{BET}}\left(\text{m}^2\ \text{g}^{-1}\right)} \tag{3}$$

The t-plot and BJH methods were used to measure the micropore surface area (S_{mi}) and micropore volume (V_{mi}) as well as the mesopore surface area (S_{mes}) and mesopore volume (V_{mes}) of biochar using the BELSORP analysis program software. Pore size distribution is calculated from desorption isotherm by applying the BJH method [36].

2.4.2. Microscopy

The surface morphology of the biochar samples was analyzed by the SEM (QUANTA 250, Czechoslovakia) which was coupled with EDAX to carry out an elemental analysis.

2.4.3. FTIR spectroscopy of the biochar

The surface functional groups of the biochar were estimated by FTIR spectroscopy (Platinum ATR) model V-100 VERTEX70 (Germany) to detect the IR-observable functional groups on the biochar surface, in the wavenumber 400–4,000 cm^{-1}.

2.4.4. Thermogravimetric analysis (TGA), differential thermal analysis (DTA) and differential scanning calorimetry (DSC)

Thermal analyses were performed using an SDT650-simultaneous thermal analyzer instrument in the range from 60°C to 1,000°C using 5°C per min as ramping temperature.

2.5. Theoretical background

2.5.1. Theory-equilibrium isotherms

The Langmuir model [37] assumes uniform energies of adsorption of a solute from a liquid solution onto a surface containing a definite number of identical sites as monolayer adsorption and no transmigration of adsorbate in the plane of the surface [38]. The linear equation of the Langmuir model was reported as Eq. (4):

$$\frac{C_e}{q_e} = \frac{1}{K_a Q_m} + \frac{1}{Q_m} \times C_e \tag{4}$$

where Q_m reflected complete monolayer adsorption (mg g^{-1}); K_a is a constant (L mg^{-1}) related to the energy of adsorption.

The linear equation of the Freundlich model [39] can be written as Eq. (5):

$$\log q_e = \log K_F + \frac{1}{n}\log C_e \quad (5)$$

where K_F is the relative adsorption capacity and $1/n$ is the intensity of the adsorption constant referring to surface heterogeneity which becoming more heterogeneous as its value gets closer to zero. A value for $1/n < 1$ indicates a normal Langmuir isotherm while $1/n > 1$ is indicative of cooperative adsorption. The maximum adsorption capacity can be calculated according to Halsey [40] Eq. (9). The maximum adsorption capacity of Freundlich (Q_m, mg g^{-1}) can be measured from Eq. (6).

$$Q_m = K_F C_0^{1/n} \quad (6)$$

The linear equation of the Temkin isotherm model [41] which assumed that the heat of adsorption of all the molecules in the layer decreases linearly with coverage due to adsorbent–adsorbate interactions [42] can be presented as Eq. (7) [43–45].

$$q_e = \beta \ln A + \beta \ln C_e \quad (7)$$

where $\beta = (RT)/b$, T is the absolute temperature in Kelvin and R is the universal gas constant, 8.314 J mol^{-1} K^{-1}. The constant b is related to the heat of adsorption [46,47].

2.5.2. Adsorption kinetics

The linear equation of the Lagergren first-order model [48], which is the earliest known equation studied the adsorption rate based on the adsorption capacity, is generally expressed as Eq. (8).

$$\log\left(q_e - q_t\right) = \log\left(q_e\right) - \frac{k_1}{2.303}t \quad (8)$$

The relation between $\log(q_e - q_t)$ and t should give a linear relationship if the reaction rate is first-order and from the slope and intercept of the plot, respectively, we can measure k_1 and predicted q_e.

The pseudo-second-order model given by Ho et al. [49] as linear Eq. (9).

$$\left(\frac{t}{q_t}\right) = \frac{1}{k_2 q_e^2} + \frac{1}{q_e}\left(t\right) \quad (9)$$

The initial sorption rate, h, may be calculated from Eq. (10).

$$h = k_2 q_e^2 \quad (10)$$

If the second-order kinetics is applicable, then the relation between t/q_t and t should show a linear relationship from which the values of k_2 and q_e, respectively, can be calculated from the intercept and slope.

The linear form of the Elovich kinetic model is generally expressed as Eq. (11) [50–52].

$$q_t = \frac{1}{\beta}\ln\left(\alpha\beta\right) + \frac{1}{\beta}\ln\left(t\right) \quad (11)$$

If the Elovich model is applicable the relation between q_t and $\ln(t)$ should give a linear relationship with a slope of $(1/\beta)$ and an intercept of $(1/\beta) \times \ln(\alpha\beta)$.

The possibility of intraparticle diffusion [53,54] is explored by using Eq. (12).

$$q_t = K_{\text{dif}} t^{1/2} + C \quad (12)$$

where C is constant give information about the thickness of the boundary layer and can be measured from the intercept. K_{dif} is a constant directly calculated from the slope of the regression line and refers to the intraparticle diffusion rate. The resistance to the external mass transfer increase as the C value increase.

3. Results and discussion

3.1. Characteristics of biochars

3.1.1. Fourier-transform infrared spectroscopy

The FTIR spectra of raw Pea-peel and the four pea biochars are presented in Figs. 1 and 2. The strong band at 3,224–3,378 cm^{-1} represents the O–H stretching vibration, and existed in Pea-peel, Pea-B, and Pea-BO biochars, while the broad adsorption peak around 3,169 and 3,221 cm^{-1} is inductive of the existence of the –OH group of glucose and the –NH of the amino group in Pea-BO-NH_2 and Pea-BO-TETA biochars (Fig. 2). The appearance of this new band indicated the introduction of an amino group into the surface of the biochars. The peak at 2,919–2,929 cm^{-1} is assigned to –CH stretching vibration and existed in Pea-peel and the four pea biochars. The adsorption peak at 1,701 cm^{-1} can be assigned to C=O stretching of the carboxyl group which was existed in Pea-B and Pea-BO and it is completely disappeared in Pea-peel, Pea-BO-NH_2, and Pea-BO-TETA (Figs. 1 and 2). However, the strength at 17,01 cm^{-1} of Pea-BO biochar was enhanced when compared with Pea-B biochar, indicating the C=O functional group might be increased by O_3 treatment. The band at 1,620 cm^{-1} implies the C=O stretching vibration and almost existed in Pea-peel, Pea-B, and Pea-BO biochars. Similarly, Pea-peel represented a strong peak at 1,620 cm^{-1} than Pea-B and Pea-BO biochars, suggesting the sulfuric acid and ozonation might induce less C=O functional group than raw Pea-peel. N-H stretching vibration in fatty amine or aromatic secondary amine was only appeared at 1,561 and 1,567 cm^{-1} in Pea-BO-NH_2 and Pea-BO-TETA, respectively, indicating NH_4OH and TETA modification might increase the N–H functional group of Pea-BO-NH_2 and Pea-BO-TETA. The peak at 1,414–1,436 cm^{-1} represents that the C–O functional group was weak and appeared only in Pea-peel, Pea-B, and Pea-BO. The adsorption band at 1,360–1,378 cm^{-1} was assigned to the –N=C=O group stretching vibration. These new band resulting from nitrogen-containing functional

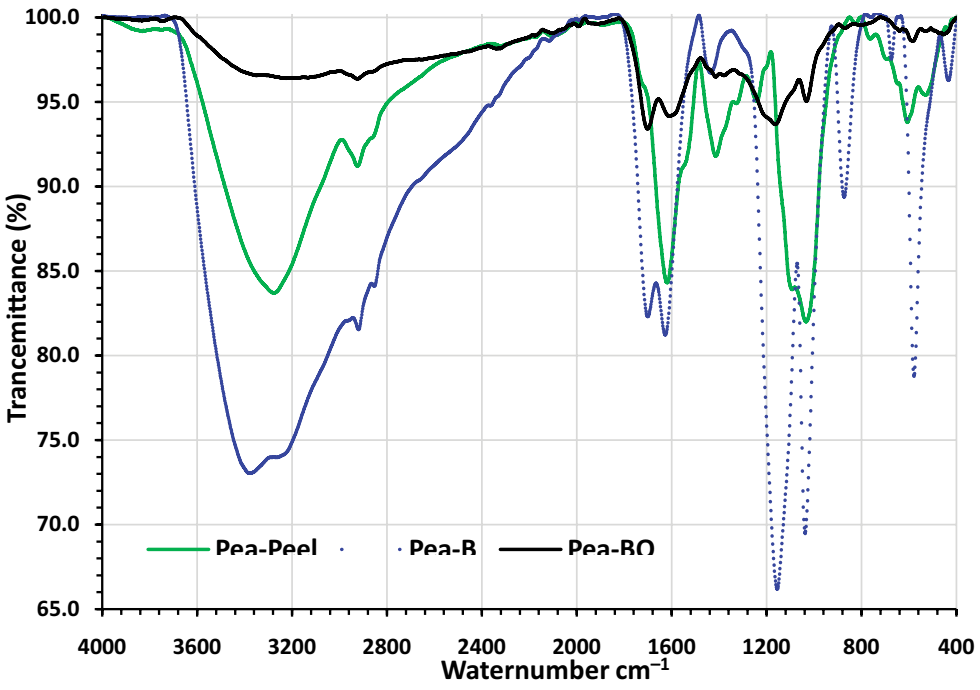

Fig. 1. FTIR analysis of Pea-peel, Pea-B, and Pea-BO.

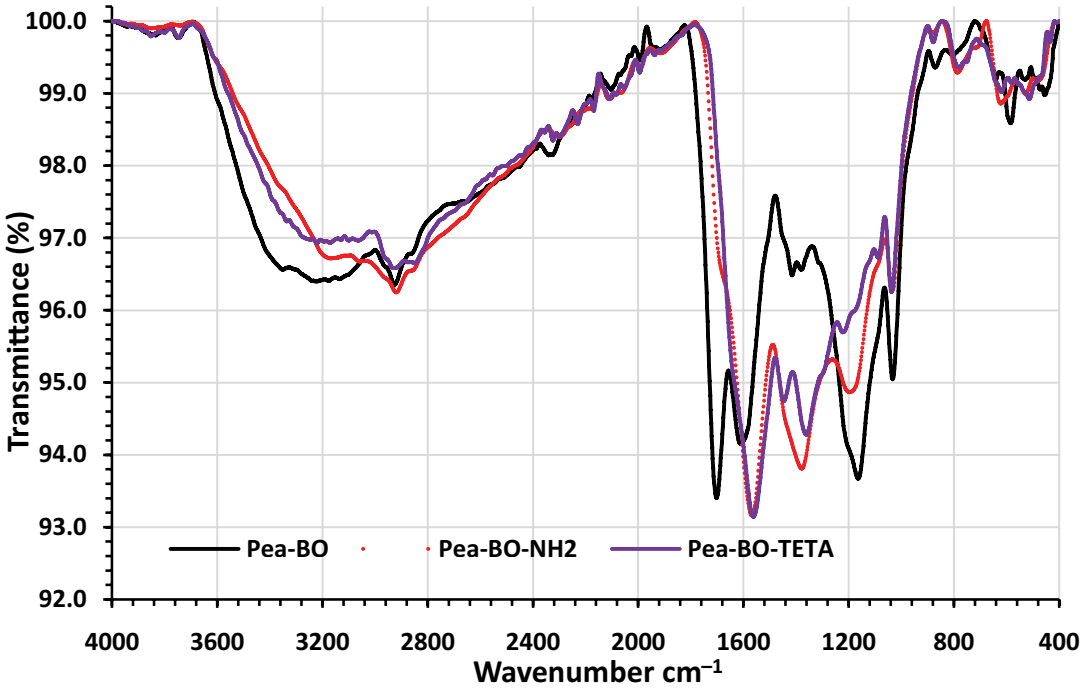

Fig. 2. FTIR analysis of Pea-BO, Pea-BO-NH_2, and Pea-BO-TETA.

groups appeared on Pea-BO-NH_2 and Pea-BO-TETA, proved that the new amino groups were successfully introduced to the biochar surface after the treatment. The presence of oxygenated carbon chains peak at 1,239–1,155 cm^{-1} represents an increase of C–O–C asymmetric stretching functional group for Pea-B and Pea-BO, while it is decreased in Pea-peel, Pea-BO-NH_2 and Pea-BO-TETA biochars. The band at 1,032–1,037 cm^{-1} represents that the C–O–H functional

group existed in all biochars while it is strong in raw Pea-peel. Furthermore, it seems there was a notable difference between Pea-peel and the four prepared biochars in the band strength at 1,032–1,037 cm^{-1}, indicating NH_4OH and TETA modification could have effect on the C–O–H functional group of biochars.

3.1.2. Determination of textural properties

The textural properties were calculated by the BET and BJH methods including the surface area, total pore volume, mean pore diameter, monolayer volume, mesopore area, mesopore volume, and mesopore distribution peak for the Pea-B, Pea-BO, Pea-BO-NH_2, and Pea-BO-TETA biochars and are presented in Fig. 3. As shown in Fig. 3, the BET – specific surface area of biochars declined as Pea-B (21.63 m^2 g^{-1}) > Pea-BO (12.87 m^2 g^{-1}) > Pea-BO-TETA (11.86 m^2 g^{-1}) > Pea-BO-NH_2 (11.02 m^2 g^{-1}). It was noted that the ozonation and amination reactions reduced the specific surface area of Pea-BO, Pea-BO-NH_2, and Pea-BO-TETA biochars. The monolayer volume values of Pea-B, Pea-BO, Pea-BO-TETA, and Pea-BO-NH_2 biochars were 4.97, 2.96, 2.73, and 2.53 cm^3 g^{-1}, respectively, which showed a similar trend with the specific surface area. The total volume values of Pea-B, Pea-BO, Pea-BO-NH_2, and Pea-BO-TETA biochars were 0.025, 0.026, 0.024, and 0.029 cm^3 g^{-1}, respectively. The mean pore diameters of Pea-B, Pea-BO, Pea-BO-NH_2, and Pea-BO-TETA biochars were 4.56, 8.17, 8.67, and 9.88 nm (mesopores), respectively. This result proved that the modification process enlarged the pore size of Pea-BO, Pea-BO-NH_2, and Pea-BO-TETA, especially Pea-BO-TETA biochar. The meso surface area of biochars declined as Pea-B (20.47 m^2 g^{-1}) > Pea-BO (15.43 m^2 g^{-1}) > Pea-BO-TETA (14.32 m^2 g^{-1}) > Pea-BO-NH_2 (13.05 m^2 g^{-1}). It was also noted that the modification reactions reduced the specific surface area of Pea-B biochar. The mesopore volume values of Pea-BO-TETA, Pea-B, Pea-BO, Pea-BO-TETA, and Pea-BO-NH_2 biochars were 0.031, 0.029, 0.028, and 0.026 cm^3 g^{-1}, respectively. The mesopore distribution peak values of Pea-B was 1.66 nm while it was 1.22 for Pea-BO, Pea-BO-NH_2, and Pea-BO-TETA biochars, respectively. The specific surface area, total pore volume was decreased after functionalization may be due to the blockage of the pore. The empty pores available in un-modified Pea-B biochar have been blocked by the amine functional groups in Pea-BO, Pea-BO-NH_2, and Pea-BO-TETA biochars. However, there is an increase in the mean pore diameter after the amine modification process, which may be explained by filling the small pores.

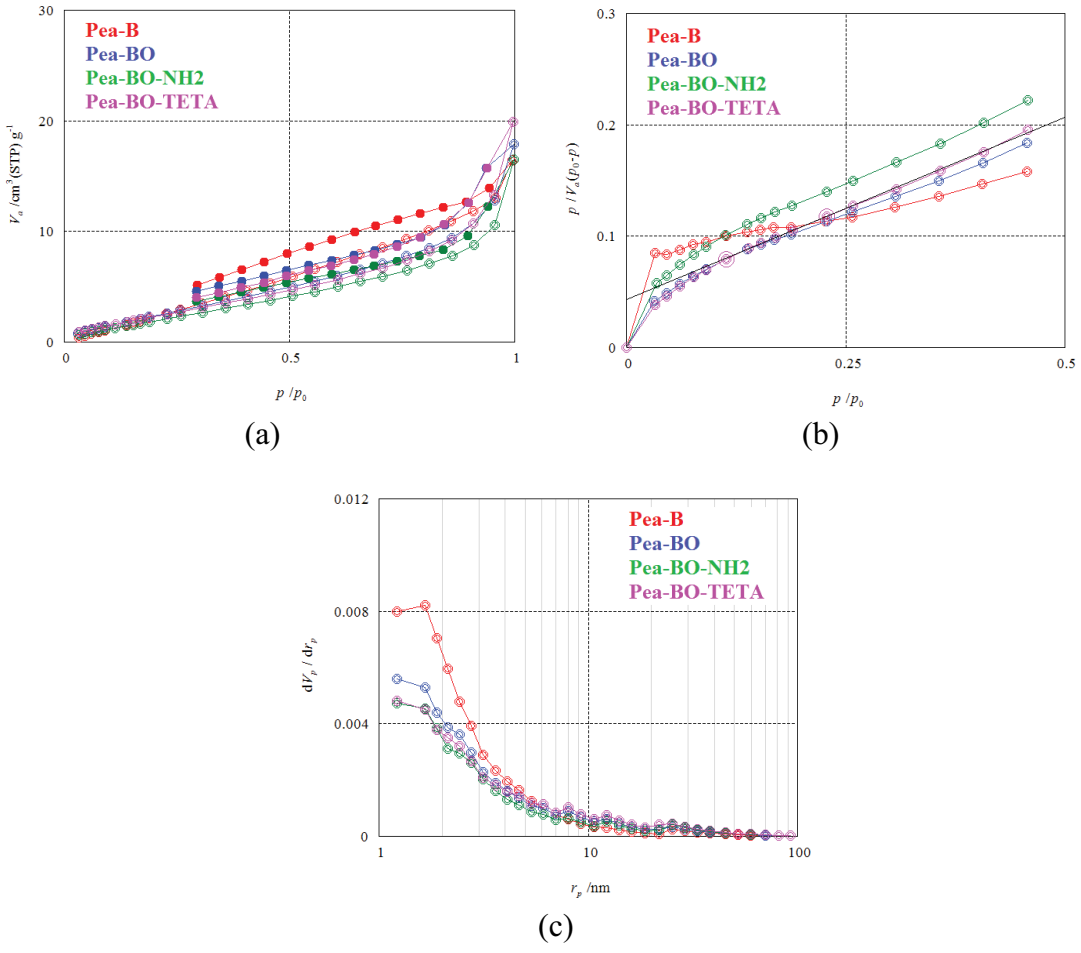

Fig. 3. (a) Adsorption desorption plot, (b) BET analysis plot, and (c) of Pea-B, Pea-BO, Pea-BO-NH_2, and Pea-BO-TETA biochars.

3.1.3. Scanning electron microscopy

SEM micrographs of raw Pea-peel, Pea-B, Pea-BO, Pea-BO-NH_2, and Pea-BO-TETA biochars were examined (Fig. 4). Fig. 4b shows the porous structure of Pea-B biochar with different size indicating relatively high surface. Fig. 4c of Pea-BO biochar shows, there was no deformation of the pores have occurred after ozonation. Figs. 4d and e show the surface morphology of Pea-BO-NH_2, and Pea-BO-TETA biochars, respectively. SEM images of Pea-BO-NH_2 and Pea-BO-TETA biochars show that most of their pores and caves

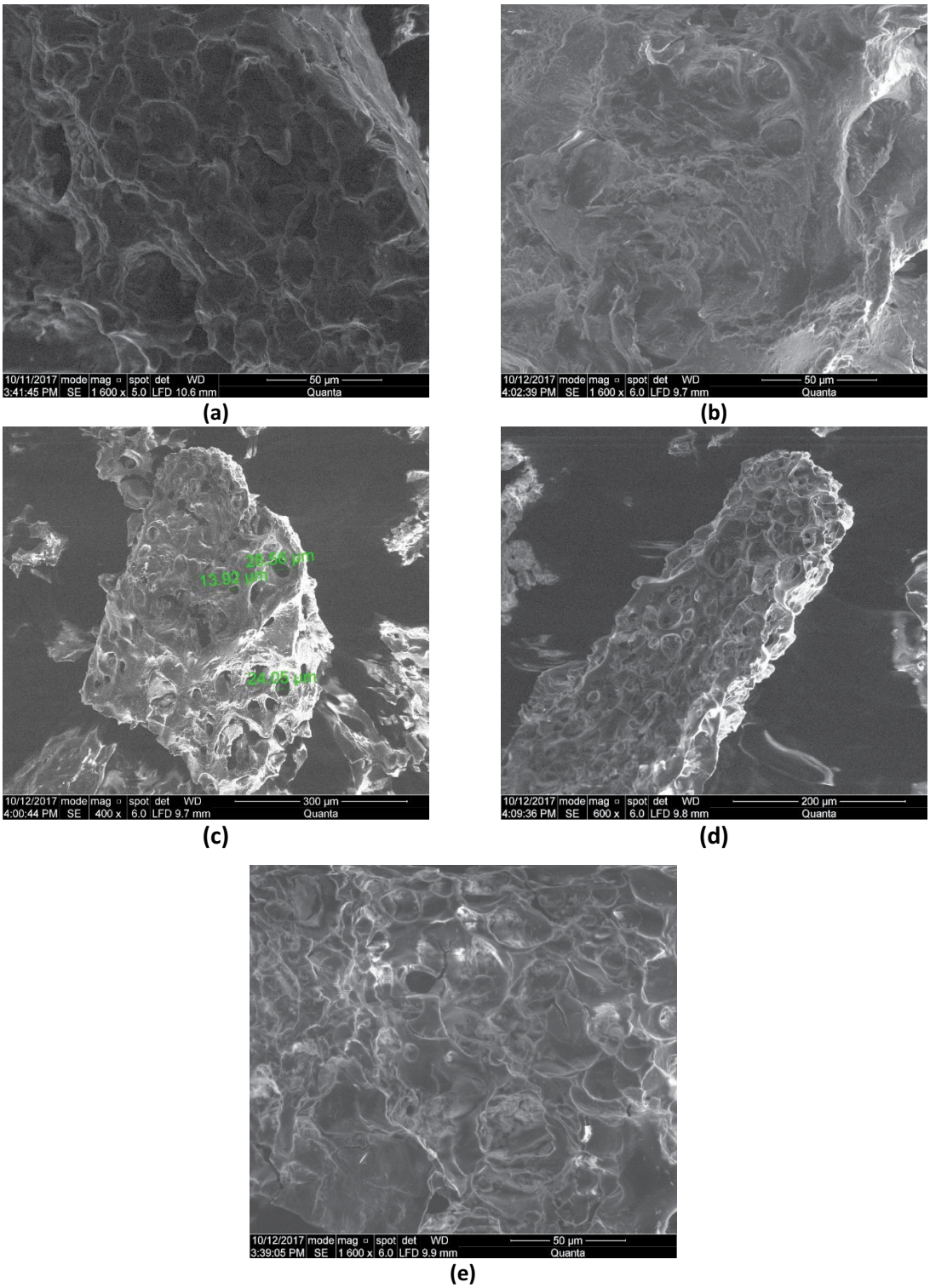

Fig. 4. SEM image of Pea-peel (a), Pea-B (b), Pea-BO (c), Pea-BO-NH_2 (d), and Pea-BO-TETA (e).

had been blocked after the introduction of the amine to create active sites for adsorption.

Chemical compositions of the samples were analyzed with EDAX. This analysis was carried out for the pea modified and unmodified biochars. The chemical compositions of Pea-B and Pea-BO biochars are reported in Table 1. Table 1 shows the absence of nitrogen before the modification by NH_4OH and TETA reagents. The EDAX analysis of Pea-BO-NH_2 and Pea-BO-TETA biochars proved the presence of about 12.48% and 19.24% sample weight for nitrogen element, respectively.

3.1.4. Thermal analysis

Fig. 5 illustrates the thermogravimetric profile of the raw material Pea-peel, Pea-B, Pea-BO, Pea-BO-NH_2, and Pea-BO-TETA biochars, respectively, as a function of temperature. As seen in Fig. 5, the decomposition of raw material Pea-peel, Pea-B, and Pea-BO takes place in three steps while the decomposition of the Pea-BO-NH_2 and Pea-BO-TETA biochars occurred in two steps. The first step occurred at temperatures between 50°C and 150°C due to the loss of surface-bound water and moisture present in the sample with weight loss of 4.04%, 8.78%, 3.95%, 6.13%, and 3.97%, respectively, for raw material Pea-peel, Pea-B, Pea-BO, Pea-BO-NH_2, and Pea-BO-TETA biochars. The second step with weight loss of 63.68% at 150°C–350°C, 20.53% at 150°C–275°C, 37.79% at 150°C–1,000°C, 34.97% at 150°C–1,000°C and 38.51% at 150°C–1,000°C, respectively, for raw material Pea-peel, Pea-B, Pea-BO, Pea-BO-NH_2, and Pea-BO-TETA biochars. The third step with the weight loss of 5.014% at 350°C–1,000°C and 25.70% at 275°C–1000°C, respectively, for raw material Pea-peel and Pea-B biochar. The weight remained with an order of Pea-peel < Pea-B < Pea-BO-TETA < Pea-BO < Pea-BO-NH_2 biochars and the percentages of 27.27%, 45.10%, 57.53%, 58.26%, and 58.98% were obtained which reflect more stability for oxidized and amine-modified samples than raw Pea-peel and Pea-B biochar.

DTA can be used as a method for the determination of phase diagrams, heat change measurements, and decomposition in various atmospheres (Fig. 6). The DTA curve of the Pea-peel sample exhibits two peaks at a temperature of flow T_f (76.67°C and 342.45°C), and the DTA curve of Pea-B sample exhibits two peaks at lower T_f (75.95°C and 213.84°C), which reflect that the Pea-peel maybe have higher stability than Pea-B biochar. However, the pyrolysis

Table 1
EDAX analysis data of Pea-B, Pea-BO, Pea-BO-NH_2, and Pea-BO-TETA biochars

Biochar	Pea-B		Pea-BO		Pea-BO-NH_2		Pea-BO-TETA	
Elements	Wt.%	At.%	Wt.%	At.%	Wt.%	At.%	Wt.%	At.%
C	50.57	60.44	59.28	65.74	51.24	57.59	51.16	57.07
O	34.24	30.73	40.20	34.00	35.75	30.16	28.24	24.26
N	ND	ND	ND	ND	12.48	12.03	19.24	24.26
S	11.68	5.23	0.52	0.21	0.53	0.22	0.64	0.27

ND: not detected.

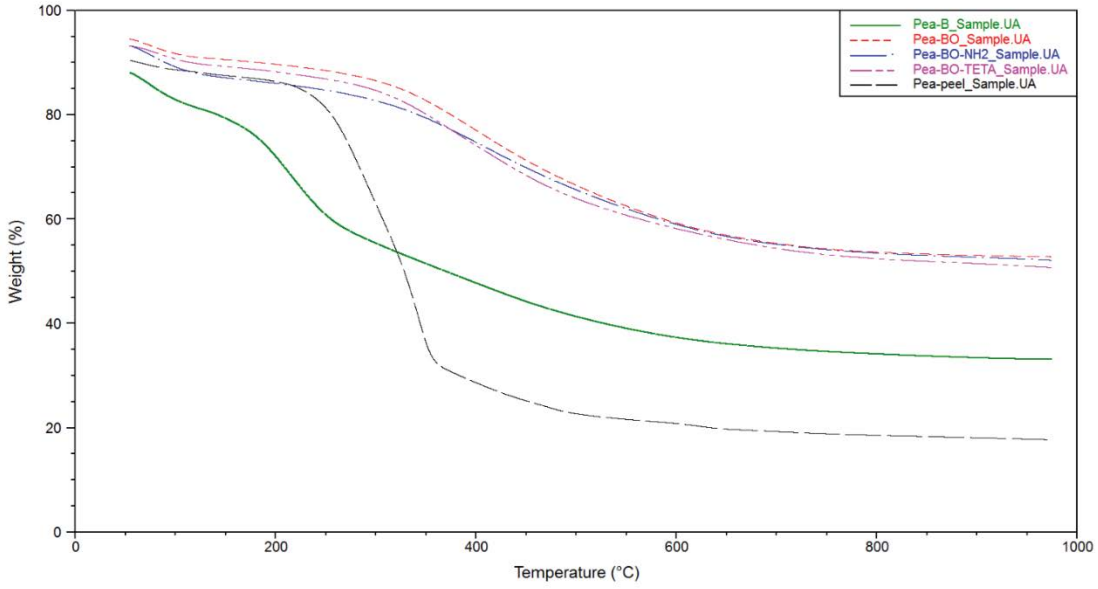

Fig. 5. TGA analysis of raw Pea-peel and Pea-B, Pea-BO, Pea-BO-NH_2, and Pea-BO-TETA biochars.

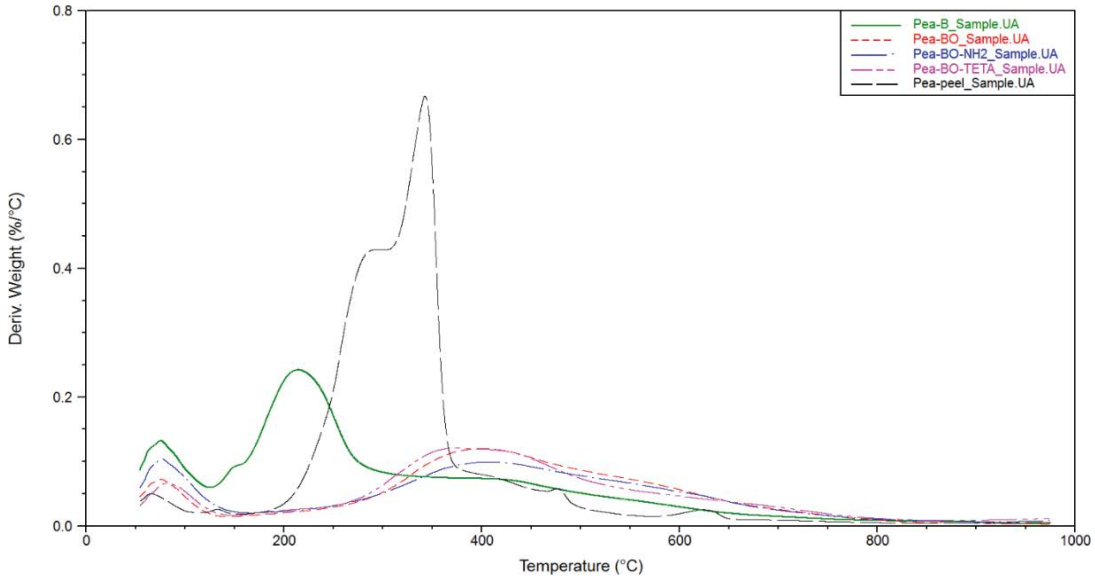

Fig. 6. DTA analysis of raw Pea-peel and Pea-B, Pea-BO, Pea-BO-NH_2, and Pea-BO-TETA biochars.

of both of Pea-peel and Pea-B samples show two well-resolved degradation peaks. The degradation peaks remain two peaks after treatment with sulfuric acid. These results imply that the degree of degradation of the Pea-peel is decreased after acid treatment dehydration. The DTA analysis of the Pea-BO, Pea-BO-NH_2 and Pea-BO-TETA samples showed manly similar two well-resolved degradation peaks at a temperature of flow T_f (76.60°C and 400.97°C), (76.73°C and 408.76°C), and (83.47°C and 374.25°C), respectively, and onset points at (56.17°C and 271.13°C), (56.23°C and 253.11°C), (56.35°C and 260.33°C), respectively. This proved that the stability of Pea-B biochar samples increased by modification with ozone and amine.

DSC can be utilized to compare materials via thermal transitions. Fig. 7 shows the DSC of raw Pea-peel and Pea-B, Pea-BO, Pea-BO-NH_2, and Pea-BO-TETA biochars. All samples showed their crystallization temperatures T_C before 100°C which are attributed to crystallization of water molecules. The DSC of the raw material of Pea-peel showed a crystallization temperature T_C at 348.29°C and 758.59°C. The DSC of Pea-B showed a crystallization temperature T_C at 219.84°C. Pea-BO, Pea-BO-NH_2, and Pea-BO-TETA biochars, respectively do not exhibit other phase transitions.

3.2. Adsorption of AO7 dye

3.2.1. Effect of pH

Adsorption process for the removal of dyes from wastewater is pH-dependent in which the pH plays an important and influencing factor in the adsorption process. The pH effect on the AO7 dye adsorption capacity of Pea-B, Pea-BO-NH_2, and Pea-BO-TETA biochars was studied at varied pH range from 2 to 9. From Fig. 8a, it is observed that the highest efficiency of removal was obtained at pH 2 as percentage removal of AO7 dye ranged between 96% and 99%. By increasing pH from 2 to 5.5, the percentage removal of dye is dramatically reduced from 99% to 80% for Pea-BO-NH_2, from 98% to 78% for Pea-BO-TETA and from 96% to 75% for Pea-B biochars. After reaching to neutral pH value, percentage removal was highly reduced. The percentage removal was 65% for Pea-BO-NH_2, 63% for Pea-BO-TETA, and 60% for Pea-B biochars. The percentage of removal has a low reductive trend with increasing pH values from 7 to 9.

Fig. 8b shows the relationship between the amounts of AO7 dye adsorbed at equilibrium (q_e) (mg g^{-1}) and the pH values variation from 2 to 9. The results indicated that, at different pH values, the q_e for the Pea-BO-NH_2 and Pea-BO-TETA biochars were nearly similar. By changing pH values from 2 to 9, the q_e decreased from 98.5 to 63 mg g^{-1} for the Pea-BO-NH_2 and Pea-BO-TETA biochars. For Pea-B biochar, the q_e at pH 2 was 19.23 mg g^{-1} and decreased to 11.45 mg g^{-1} at pH 9.

After treatment of Pea-BO biochar with NH_4OH and TETA, the percentage of removal and the amounts of dye adsorbed at equilibrium obviously enhanced, although the adsorbent dose of Pea-B biochar is four times greater than the adsorbent doses of Pea-BO-NH_2 and Pea-BO-TETA biochars (Fig. 8). The results indicated that the NH_4OH and the TETA can be used as reagents to modify Pea-BO biochar to produce highly efficient adsorbents to remove AO7 dye from wastewater. However, it must also be mentioned that the adsorption process of AO7 dye onto the surface of an adsorbent is primarily influenced by the charge on the adsorbent surface, which actually is influenced by the solution pH. The enhanced of AO7 dye adsorption by modified biochars could be attributed to the increasing of surface NH_2 content which was confirmed by its FTIR spectra and EDAX. Firstly, acid dye gives negatively charged ions when dissolved in water. At the acidic medium, the number of positively charged sites on the sorbent increase due to the presence of an excess of H^+ ions which tended to absorb onto the surface of biochar, then the dye anions will be adsorbed on the surface of adsorbent due to electrostatic attraction. While at the alkaline medium,

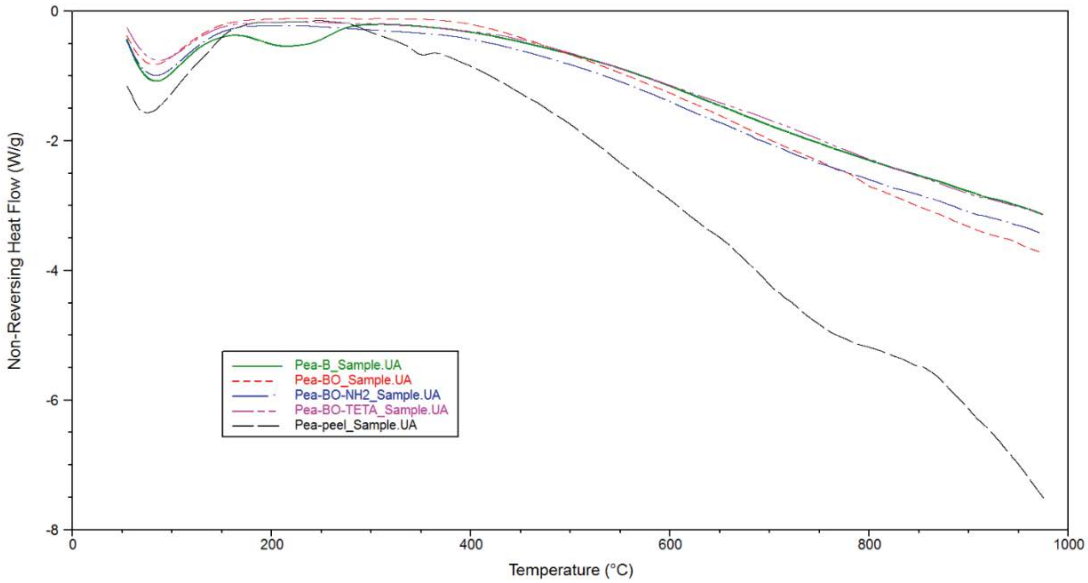

Fig. 7. DSC analysis of raw Pea-peel and Pea-B, Pea-BO, Pea-BO-NH_2, and Pea-BO-TETA biochars.

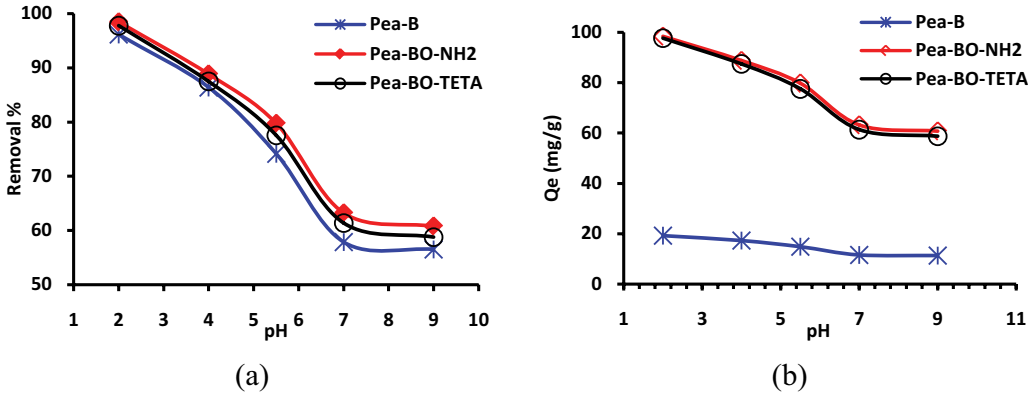

Fig. 8. Effect of solution pH value on the (a) removal % and (b) q_e (mg g^{-1}) of AO7 dye (100 mg L^{-1}) using Pea-B, Pea-BO-NH_2, and Pea-BO-TETA of adsorbent dose (5.0, 1.0, and 1.0 g L^{-1}, respectively) at 25°C ± 2°C.

there was an excess of HO^- ions which competing with the dye anions in the solution for adsorption sites. Also, in the alkaline medium, the surface sites on the biochar were negatively charged which did not favor the adsorption of anionic AO7 dye due to electrostatic repulsion. The above results showed that the formation of charge on the biochar surface is the main factor that affects the dye removal from its solution.

3.2.2. *Effect of contact time*

The contact time required achieving a specific removal of AO7 dye and it is important for applying biochar to AO7 dye adsorption applications. Fig. 9a shows the percentage removal of AO7 dye at different initial dye concentrations ranged from 75 to 200 mg L^{-1} at pH 2 using Pea-B adsorbent biochar dose (2.0 g L^{-1}) at different contact times (5–200 min). As can be observed from Fig. 9a, the percentage of removal of AO7 dye at an initial concentration (75 and 100 mg L^{-1}) was about 50% after 15 min. The percentage of removal of AO7 dye increases with an increase in time and reaches a maximum (90 %) after 3 h. At initial concentration (150 and 200 mg L^{-1}), within the first 15 min, about 70% of AO7 dye was removed and after that, the uptake of AO7 dye became slower and does not make a high change with increasing time. The optimum time to attain the equilibrium was 3 h.

Fig. 9b shows the percentage of AO7 dye removal at different initial dye concentrations ranged from 100 to 300 mg L^{-1} and pH 2 using Pea-BO-NH_2 adsorbent dose (2.0 g L^{-1}) at different contact times (5–180 min). With the beginning of adsorption contact time, the removal of AO7 dye increases quickly and reaches about 85%, after 15 min, most of the AO7 dye is removed and reaches nearly a complete removal at 3 h. The effect of contact time on the percentage of removal of AO7 dye using Pea-BO-TETA (2.0 g L^{-1}) was illustrated in Fig. 9c. It is clear from Fig. 9c that, the percentage of removal trend of AO7 dye on Pea-BO-TETA biochar for all cases was speedy within the first 15 min. The removal of the dye was 90% just after 15 min.

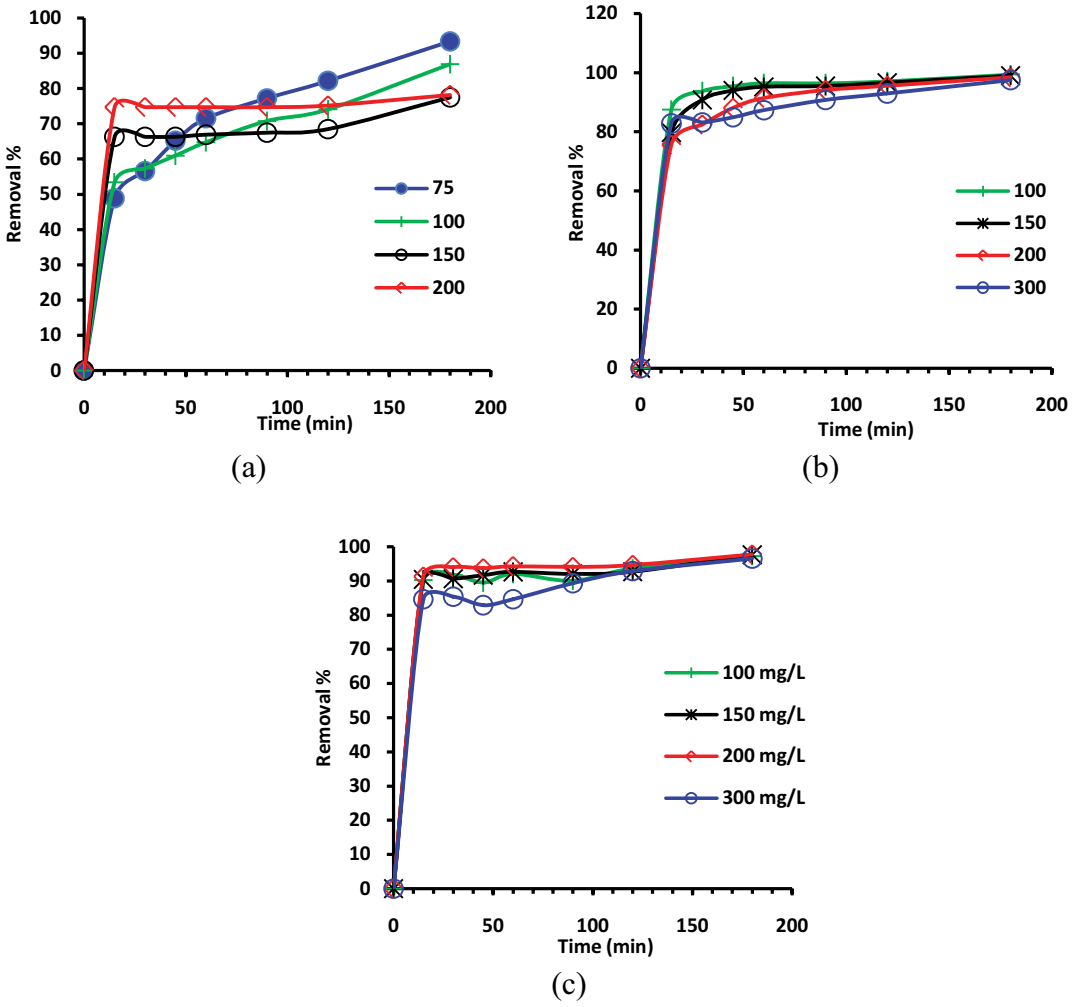

Fig. 9. (a) Removal of AO7 (75–200 mg L^{-1}) using Pea-B adsorbent dose (2.0 g L^{-1}); removal of AO7 dye (100–300 mg L^{-1}) using (b) Pea-BO-NH_2 adsorbent dose (2.0 g L^{-1}), and (c) Pea-BO-TETA adsorbent dose (2.0 g L^{-1}) at 25°C ± 2°C.

The percentage of AO7 dye removal slightly increases with time for most cases except for AO7 dye at 200 mg L^{-1} where the percentage of removal became nearly constant (about 90%). Complete removal was achieved using 2.0 g L^{-1} of adsorbent dose at 180 min for AO7 dye.

From Fig. 9, we can observe that there was rapid adsorption occurred at initial contact time (15 min) by using Pea-B, Pea-BO-NH_2, and Pea-BO-TETA biochars, but the most notable difference between the three biochars was the significantly higher removal of AO7 dye using small doses of Pea-BO-NH_2 and Pea-BO-TETA biochars at short time. After modification of Pea-B biochar by treatment with O_3 in H_2O for 2 h followed by reflux in 25% NH_4OH solution or reflux in TETA, the surface area, and pore size distribution may not be the functions of AO7 dye adsorption because they were slightly changed than would be expected based on BET analysis. The significant difference between the three biochars could be attributed to surface modification. One hypothesis is the amine sites formation on the surface of biochars during the modification process. Amine sites produced a great chemical affinity between the AO7 dye and the modified biochar. The slow rate of dye adsorption reported after the first 15 min may be attributed to the slow pore diffusion of the dye ions into the bulk of biochar adsorbents.

3.2.3. *Effect of initial concentration*

The influence of the initial dye concentration on the percentage of removal and adsorption capacity at equilibrium (q_e) was investigated. The process was carried out at adsorbent doses using Pea-B biochar (2, 3, 4, 5, and 6 g L^{-1}) in the test solution, pH 2 at a different initial concentration of AO7 dye (75, 100, 150, and 200 mg L^{-1}) for 3 h at room temperature (25°C ± 2°C) (Fig. 10a). The results indicate that the percentage of removal of AO7 dye decreases as the initial concentration of dye increased. The percentage of removal of AO7 dye decreased from 94% to 79%, 97% to 89%, 98% to 93%, 99% to 96% and 99% to 97% with an increased in the initial dye concentration from 75 to 200 mg L^{-1} using different Pea-B doses of 2, 3, 4, 5, and 6 g L^{-1}, respectively. Fig. 10b shows that, the values of q_e decrease with an increase of

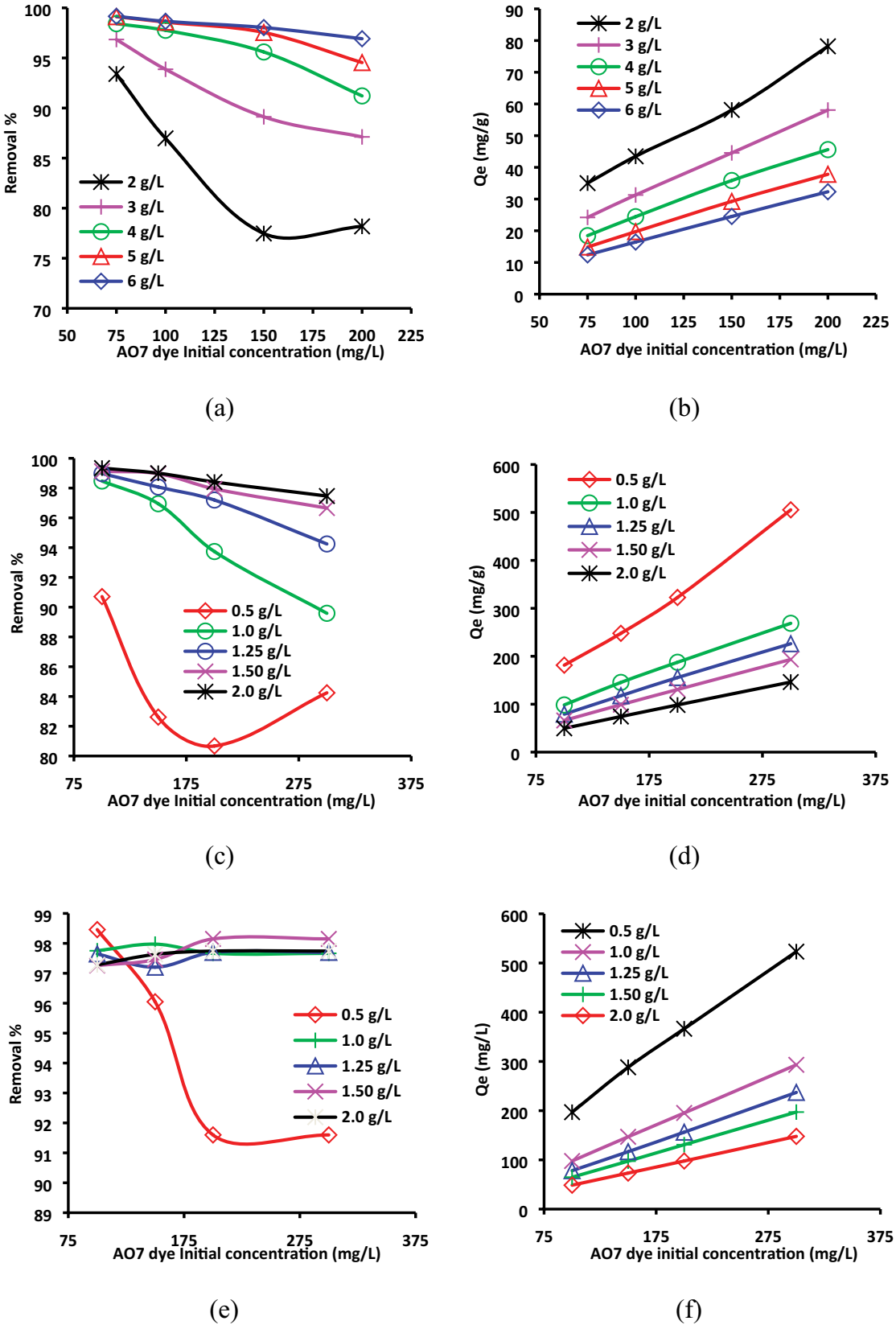

Fig. 10. Effect of AO7 dye initial concentration (75–200 mg L^{-1}) on its (a) removal %, (b) q_e (mg g^{-1}) using different Pea-B doses (2–6 g L^{-1}); effect of AO7 dye initial concentration (100–300 mg L^{-1}) on its (c) removal %, (d) q_e (mg g^{-1}) using different Pea-BO-NH_2 doses (0.5–2.0 g L^{-1}), (e) removal %, and (f) q_e (mg g^{-1}) using different Pea-BO-TETA doses (0.5–2.0 g L^{-1}) at 25°C ± 2°C.

Pea-B doses at the same initial concentration of AO7 dye, while it increases with an increase of initial dye concentration for all studied doses of Pea-B as adsorbent.

The adsorption experiments at an initial concentration of AO7 dye from 100 to 300 mg L^{-1} on its removal % using different Pea-BO-NH_2 doses (0.5–2.0 g L^{-1}) were also performed for 3 h at pH 2, 25°C ± 2°C and the results are represented in Fig. 10c. It is observed that the percentage of removal increased with increasing of mass concentration of Pea-BO-NH_2 adsorbent from 0.5 to 2.0 g L^{-1}. The percentage of removal decreased from 91 to 81% for an increase in the initial concentration of AO7 dye from 100 to 200 mg L^{-1} using 0.5 g L^{-1} of Pea-BO-NH_2 biochar, then, the percentage of removal increases to 84% at an initial concentration of dye 300 mg L^{-1} using 0.5 g L^{-1} of Pea-BO-NH_2 biochar, whereas the percentage of removal of dye decreases as the initial concentration of dye increased. The percentage of removal of dye decreased from 98.5% to 90% for an increase in the initial concentration of AO7 dye from 100 to 300 mg L^{-1} using absorbent dose 1.0 g L^{-1} of Pea-BO-NH_2 adsorbent. Also, the percentage of removal of AO7 dye decreased from 99 to 95% for the same increase in the initial concentration of AO7 dye from 100 to 300 mg L^{-1} using the absorbent dose 1.25 g L^{-1} of Pea-BO-NH_2 adsorbent. The percentage of removal of dye decreased from 99% to 98% and from 100% to 99% for the same increase in the initial concentration of AO7 dye from 100 to 300 mg L^{-1} using Pea-BO-NH_2 absorbent doses 1.5 and 2.0 g L^{-1}, respectively. From Fig. 10d, the results indicate that the q_e increased from 181.42 to 505.47, 98.47 to 268.76, 79.18 to 226.19, 66.09 to 193.32 and 49.67 to 146.20 mg g^{-1} with an increase in the initial dye concentration from 100 to 300 mg L^{-1} using Pea-BO-NH_2 doses 0.5–2.0 g L^{-1}, respectively. The adsorption experiments at initial concentration ranged between 100 and 300 mg L^{-1} using different Pea-BO-TETA adsorbent doses (0.5–2.0 g L^{-1}) were also performed for 3 h at 25°C ± 2°C, at pH 2 to study their effects on the removal percent of AO7 dye and the results are represented in Fig. 10e. It is shown that the percentage of removal of dye decreased from 98.5% to 91.5% for an increased in the initial concentration of dye from 100 to 200 mg L^{-1} and after that, there was a slightly increased to 92% at an initial concentration of dye 300 mg L^{-1}, using 0.5 g L^{-1} Pea-BO-TETA adsorbent dose, where the percentage of removal of AO7 dye slightly increases from about 97.5% to 98.5% with increased of mass concentration of adsorbent from 1.0 to 2.0 g L^{-1}. From Fig. 10f, the results indicate that the q_e increased from 196.92 to 523.12, 97.75 to 293.17, 78.12 to 237.09, 64.84 to 197.16 and 48.64 to 147.81 mg g^{-1} with an increase in the initial dye concentration from 100 to 300 mg L^{-1} using Pea-BO-TETA doses 0.5, 1, 1.25, 1.5, and 2.0 g L^{-1}, respectively.

The q_e onto the three different biochars (Pea-B, Pea-BO-NH_2, and Pea-BO-TETA) at a lower initial concentration of AO7 dye were smaller than the corresponding q_e at higher initial concentrations. The decrease in q_e value was probably due to the concentration gradient between the adsorption vacant sites of the solid adsorbent and the concentration of dye solutions gets decreased with increasing adsorbent mass leading to decrease in q_e value or during the sorption process, there was an aggregation took place to lead to a reduction in surface area of the adsorbent. The increase in the q_e, although using small doses of Pea-BO-NH_2 and Pea-BO-TETA (0.5 g L^{-1}) and at a high initial concentration of dye was significant. The q_e increased to about seven times by using Pea-BO-NH_2 and Pea-BO-TETA as adsorbent than using of Pea-B as adsorbent. This notable result may be attributed to the formation of reactive amino groups on the surface of biochars during the modification process that efficiently increased the negative surface charges.

3.2.4. Effect of adsorbent dosage

The experimental conditions are represented in Fig. 11. The experimental results revealed that the percentage of removal of AO7 dye increased gradually with increasing doses of the adsorbent, while the q_e decreased with increasing of the adsorbent doses for all studied Pea-B doses. Increasing the quantity of Pea-B doses from 2 to 6 g L^{-1} significantly enhanced the percentage of removal of AO7 dye from 94% to 98%, 86% to 97%, 77% to 96% and 78% to 95% for an initial dye concentration of 75, 100, 150, and 200 mg L^{-1}, respectively. On the other hand, the q_e decreased from 35 to 10, 45 to 20, 60 to 30 and 80 to 35 mg g^{-1} with increasing of the quantity of adsorbent from 2 to 6 g L^{-1} for initial dye concentration of 75, 100, 150, and 200 mg L^{-1}, respectively.

The effect of different adsorbent dosages (0.5–2.0 g L^{-1}) on AO7 dye removal and the amount of adsorption at equilibrium by using Pea-BO-NH_2 and Pea-BO-TETA biochars under similar conditions (initial concentration of dye 100, 150, 200 and 300 mg L^{-1}, adsorption time 3 h, pH 2 and 25°C ± 2°C) were studied and reported in Figs. 11c–f. The results obtained revealed that the percentage of removal of AO7 dye increased gradually with increasing doses of the adsorbent, while the q_e decreased with increasing of the quantity of adsorbent for all studied doses of the two adsorbents (Pea-BO-NH_2 and Pea-BO-TETA).

Increasing the quantity of Pea-BO-NH_2 biochar from 0.5 to 2.0 g L^{-1} significantly enhanced the percentage of removal of AO7 dye from 91% to 99%, 83% to 98%, 81% to 97.5% and 84% to 97% for an initial dye concentration of 100, 150, 200 and 300 mg L^{-1}, respectively (Fig. 11c). On the other hand, the q_e decreased from 190 to 50, 250 to 100, 320 to 120 and 525 to 190 mg g^{-1} with increasing of the initial dye concentration from 100 to 300 mg L^{-1} using adsorbent doses of 0.5, 1.0, 1.25, 1.5, and 2.0 g L^{-1}, respectively (Fig. 11d). The maximum percentage of removal and minimum q_e value was achieved using 2.0 g L^{-1} of adsorbent dose (Figs. 11c and d).

Also, increasing the quantity of Pea-BO-TETA biochar from 0.5 to 2.0 g L^{-1} enhanced the percentage of removal of AO7 dye from 93.5% to 98.5%, 92% to 98%, 91.5% to 97.5% and 85% to 97.5% for initial dye concentration at 100, 150, 200 and 300 mg L^{-1}, respectively (Fig. 11e). The q_e decreased from 200 to 60, 290 to 100, 370 to 120 and 545 to 190 mg g^{-1} with increasing of the quantity of adsorbent from 0.5 to 2.0 g L^{-1} for initial dye concentration 100, 150, 200 and 300 mg L^{-1}, respectively (Fig. 11f). The maximum percentage of removal and a minimum amount of adsorption at equilibrium was achieved using 2.0 g L^{-1} of Pea-BO-NH_2 and Pea-BO-TETA adsorbent doses. These results can be attributed to the increased availability of active adsorption sites for AO7 dye ion binding. The higher removal of dye by Pea-BO-NH_2 and Pea-BO-TETA than Pea-B biochars were caused by the synergy of amino functionality introduced by the chemical

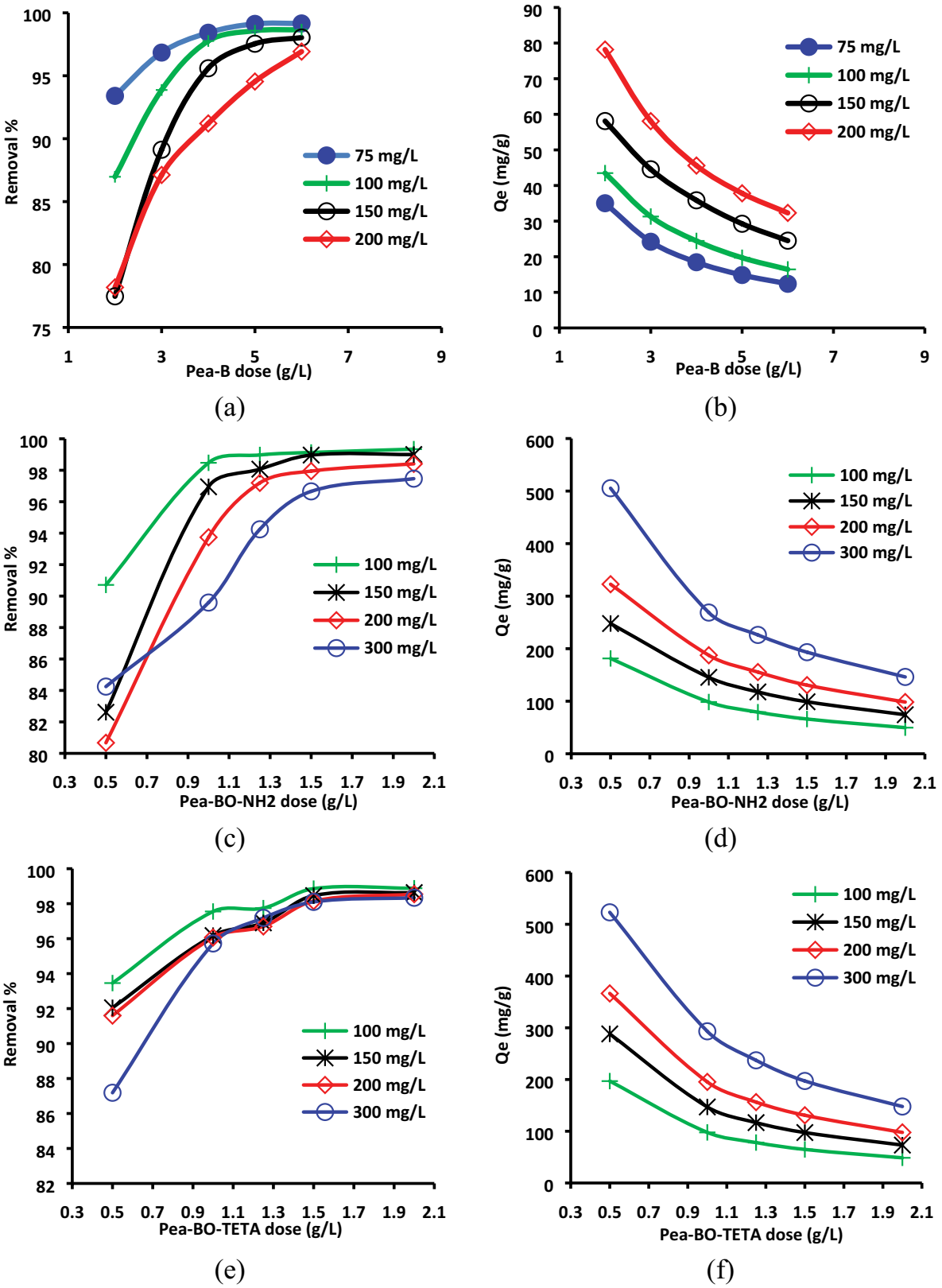

Fig. 11. Effect of Pea-B different doses (2–6 g L^{-1}) on (a) removal %, (b) q_e (mg g^{-1}) of different initial concentration (75–200 mg L^{-1}); effect of Pea-BO-NH_2 different doses (0.5–2.0 g L^{-1}) on (c) removal %, (d) q_e (mg g^{-1}) of different initial concentration (100–300 mg L^{-1}); effect of Pea-BO-TETA different doses (0.5–2.0 g L^{-1}) on (e) removal %, and (f) q_e (mg g^{-1}) of AO7 dye at 25°C ± 2°C.

modification of ozonized biochar surface with ammonium hydroxide solution and TETA. The percentage of removal of AO7 dye increased to about 99% with the increase in the adsorbent dose to 2.0 g L^{-1}. This finding suggests that the efficiency of the proposed modification to remove AO7 dye from its water solution.

3.3. Adsorption isotherms

Modeling of isotherm data is an important step to designing adsorption systems for dye removal. There are many well-established models that can be employed to investigate adsorption data of an experiment. Equation parameters of these models often provide some insight into the adsorption mechanism, the surface properties, and the degree of affinity of the adsorbents. The correlation with the amount of adsorption and the liquid-phase concentration in this work was tested with Langmuir, Freundlich, and Temkin isotherm models.

3.3.1. Langmuir isotherm

Values of Langmuir constants, the saturated monolayer sorption capacity (Q_m), and the equilibrium adsorption constant (K_L) are represented in (Table 2) for the sorption of AO7

Table 2
Isotherm study data of adsorption of AO7 dye of different initial concentration (75–200 mg L^{-1}) onto Pea-B of different adsorbent doses (2–6 g L^{-1} dye solution), isotherm study data of adsorption of AO7 dye of different initial concentration (100–300 mg L^{-1}) onto Pea-BO-NH_2 and Pea-BO-TETA of different adsorbent doses (0.5–2.00 g L^{-1}) at room temperature 25°C ± 2°C

Isotherm model	Isotherm parameter	Pea-B doses (g L^{-1}) for AO7 dye solution				
		2.0	3.0	4.0	5.0	6.0
Langmuir	Q_m (mg g^{-1})	88.49	68.49	51.55	42.74	40.98
	K_L	0.09	0.16	0.41	0.66	0.56
	R^2	0.915	0.961	0.998	0.998	0.989
Freundlich	$1/n$	0.338	0.359	0.335	0.338	0.430
	K_F ($mg^{1-1/n}$ $L^{1/n}$ g^{-1})	19.46	17.12	18.14	17.56	14.94
	Q_m (mg g^{-1})	92.34	89.37	84.78	83.43	108.22
	R^2	0.922	0.980	0.987	0.986	0.996
Temkin	A_T	1.21	2.07	5.13	8.38	5.60
	B_T	17.76	13.61	10.14	8.38	8.90
	R^2	0.851	0.934	0.999	0.995	0.981
		Pea-BO-NH_2 dose (g L^{-1})				
		0.50	1.0	1.25	1.50	2.00
Langmuir	Q_m (mg g^{-1})	416.67	303.03	263.16	238.10	185.19
	K_L	0.07	0.203	0.31	0.40	0.45
	R^2	0.945	0.979	0.991	0.982	0.981
Freundlich	$1/n$	0.545	0.324	0.374	0.415	0.435
	K_F ($mg^{1-1/n}$ $L^{1/n}$ g^{-1})	49.84	86.28	79.23	74.77	60.42
	Q_m (mg g^{-1})	612.07	384.15	443.91	504.54	448.33
	R^2	0.827	0.994	0.998	0.976	0.998
Temkin	A_T	0.27	3.42	3.82	4.29	4.84
	B_T	161.50	54.54	52.49	49.67	38.88
	R^2	0.699	0.962	0.983	0.977	0.975
		Pea-BO-TETA dose (g L^{-1})				
		0.50	1.0	1.25	1.50	2.00
Langmuir	Q_m (mg g^{-1})	588.24	344.83	303.03	312.50	333.33
	K_L	0.19	0.070	0.05	0.03	0.02
	R^2	0.997	0.998	0.993	0.991	0.980
Freundlich	$1/n$	0.294	0.944	0.955	2.26	1.82
	K_F ($mg^{1-1/n}$ $L^{1/n}$ g^{-1})	170.65	47.54	40.07	6.3314	7.80
	Q_m (mg g^{-1})	561.46	2,343.92	1,953.70	3,154.69	2,039.47
	R^2	0.987	0.985	0.963	1.000	0.987
Temkin	A_T	4.0479	0.7716	1.1235	0.452	0.4925
	B_T	96.289	168.640	105.510	254.100	149.870
	R^2	0.993	0.996	0.961	0.984	0.987

dye onto Pea-B biochar. By blotting C_e/q_e vs. C_e (Fig. 12), the $1/Q_mK_m$ and $1/Q_m$ of the Langmuir model are, respectively, obtained from the intercept and the slope of the line plot of Fig. 12. The results obtained from the Langmuir isotherm model for the removal of AO7 dye onto Pea-B biochar indicated that the Q_m (mg g^{-1}) obtained are 88.49, 68.49, 51.55, 42.74, and 40.98 mg g^{-1} using different Pea-B biochar doses of 2, 3, 4, 5, and 6 g L^{-1}, respectively (Table 2). The correlation coefficients for the linear form of Langmuir model (R^2) are ranged from 0.915 to 0.998, which showed positive evidence on the adsorption of AO7 dye onto Pea-B biochar follows the Langmuir model isotherm (Fig. 12a). Also, the applicability of the linear form of the Langmuir model was provided by the high correlation coefficient (R^2) ≥ 0.998 at 4.0 and 5.0 g L^{-1} Pea-B dose. The Q_m was 88.49 mg g^{-1} of AO7 dye onto 2.0 g L^{-1} Pea-B biochar dose. Table 1 in supplement material, represented the relation between q_e (mg g^{-1}) of AO7 dye at different initial concentrations (75, 100, 150, and 200 mg L^{-1}) obtained by batch experimental and q_e (mg g^{-1}) calculated using data from different isotherm models at different doses of Pea-B (2.0 to 6.0 g L^{-1}) at room temperature (25°C ± 2°C). Table 1 in supplement material, showed there was a great agreement between the q_e of AO7 dye adsorption obtained by batch experimental and q_e calculated using data obtained from the Langmuir isotherm model. Figs. 12b and c represented the linear relationship of the Langmuir isotherm model for Pea-BO-NH_2 and Pea-BO-TETA biochars, respectively. Table 2 represented the values of Langmuir constants, the Q_m and K_L for the adsorption of AO7 dye onto Pea-BO-NH_2 and Pea-BO-TETA biochars, respectively. The results obtained from the Langmuir isotherm model for the removal of AO7 dye onto Pea-BO-NH_2 and Pea-BO-TETA biochars indicated that the Q_m values obtained are ranged from 416.67 to 185.19 for Pea-BO-NH_2 and from 588.28 to 303.03 mg g^{-1} for Pea-BO-TETA biochars, respectively. From Table 2, the maximum correlation coefficients for the linear form of Langmuir model (R^2) ≥ 0.991 for Pea-BO-NH_2 and 0.998 for Pea-BO-TETA biochars which showed fitting and positive evidence on the adsorption of AO7 dye onto the two adsorbents biochar follow the Langmuir model isotherm.

Tables 2 and 3 in supplement materials, represented the relation between q_e of AO7 dye obtained by batch experimental at different initial concentrations (100–300 mg L^{-1}) and q_e (mg g^{-1}) calculated using data obtained from the different isotherm models using different doses (0.5–2.0 g L^{-1}) of the Pea-BO-NH_2 and Pea-BO-TETA adsorbents. There was a significant agreement between the experimental q_e of AO7 dye and calculated q_e obtained by modeled Langmuir isotherm on the various dose of both adsorbents biochar.

3.3.2. Freundlich isotherm

Freundlich isotherm model was applied to analyze the adsorption characteristics of AO7 dye on Pea-B, Pea-BO-NH_2, and Pea-BO-TETA biochars. The linear fitting parameters from the model of Freundlich isotherm are listed in Table 2. Fig. 12 represents the plot of log (q_e) vs. log (C_e) with the intercept value of logK_F and the slope of $1/n_F$, where K_F is the Freundlich constant (L g^{-1}), related to the bonding energy. In general, as the K_F value increases, the adsorption capacity of the adsorbent, for the given adsorbate, increases. It is worth to mention that the K_F increases for Pea-BO-NH_2 and Pea-BO-TETA than that for Pea-B biochars (Table 2). In the Freundlich model, it is relatively easy for adsorbent to adsorb solute when $1/n$ is less than 1. In Table 2, all $1/n$ values were less than 1, which indicated that the three adsorbents biochar were good at adsorbing of AO7 dye. Also, n_F value indicates the degree of non-linearity between solution concentration and adsorption process. The values of $n_F > 1$, indicating that adsorption of AO7 dye on the three tested biochar is a favorable physical process and the adsorption mechanism may be controlled by the physical adsorption within pores and electrostatic attraction with amine groups. The maximum correlation coefficient obtained from the Freundlich model was $R^2 > 0.9961$ for Pea-B, >0.998 for Pea-BO-NH_2, and 1.000 for Pea-BO-TETA. Based on R^2 values, the Freundlich model isotherm fitting and agree with experimental data for all prepared adsorbents. Table 2 reported the Q_m 108.22 for Pea-B, 612.07 for Pea-BO-NH_2 and 3154.69 mg g^{-1} for Pea-BO-TETA, respectively. The higher the Q_m value, the better the adsorption of AO7 dye. It is worth mention that the Q_m for Pea-B is less than the Q_m for the Pea-BO-NH_2 and for Pea-BO-TETA.

Tables 1–3 in supplement material represented the relation between q_e of AO7 dye obtained from experimental and q_e obtained from modeled Freundlich isotherm on the various doses of Pea-B, Pea-BO-NH_2, and Pea-BO-TETA, respectively. A reliable value of calculated q_e was founded in accordance with the Freundlich isotherm model for all data collection. It could be concluded that the linear fits Freundlich equation was comparable with those for the Langmuir equation. Therefore, the adsorption processes of dye on three biochars were complicating and the probability of multilayer adsorption was comparable with that of monolayer adsorption.

3.3.3. Temkin isotherm

The Temkin constants were determined (the slope A_T is Temkin isotherm equilibrium binding constant (L g^{-1}) and intercept B_T is constant related to heat of sorption (J mol^{-1})) from the linear correlation between the q_e against lnC_e. From the Temkin plot shown in Fig. 13, the following values were estimated and listed in Table 2: A_T = 1.21, 2.07, 5.13, 8.38, and 5.60 L g^{-1} and B_T = 17.76, 13.61, 10.14, 8.38, and 8.90 J mol^{-1} for Pea-B of different adsorbent doses 2, 3, 4, 5, and 6 g L^{-1}, respectively. A_T = 0.27, 3.42, 3.82, 4.29, and 4.84 L g^{-1} and B_T = 161.50, 54.54, 52.49, 49.67, and 38.88 J mol^{-1} for Pea-BO-NH_2 of different adsorbent doses 0.5, 1.0, 1.25, 1.5, and 2.0 g L^{-1}, respectively. Also, A_T = 4.04, 0.77, 1.12, 0.45, and 0.49 L g^{-1} and B_T = 96.28, 168.64, 105.51, 254.10, and 149.87 J mol^{-1} for Pea-BO-TETA of different adsorbent doses 0.5, 1.0, 1.25, 1.5, and 2.0 g L^{-1}, respectively.

The value of the heat of sorption indicating a physical adsorption process occurred. The heat of AO7 dye adsorption B_T is directly related to coverage of AO7 dye onto three biochars due to adsorbent–adsorbate interaction. It was decreased with increasing adsorbents doses, as listed in Table 2. The correlation coefficients values obtained from Temkin isotherm $R^2 > 0.999$ for Pea-B, >0.975 for Pea-BO-NH_2 and >0.996 for Pea-BO-TETA biochars. The values of R^2

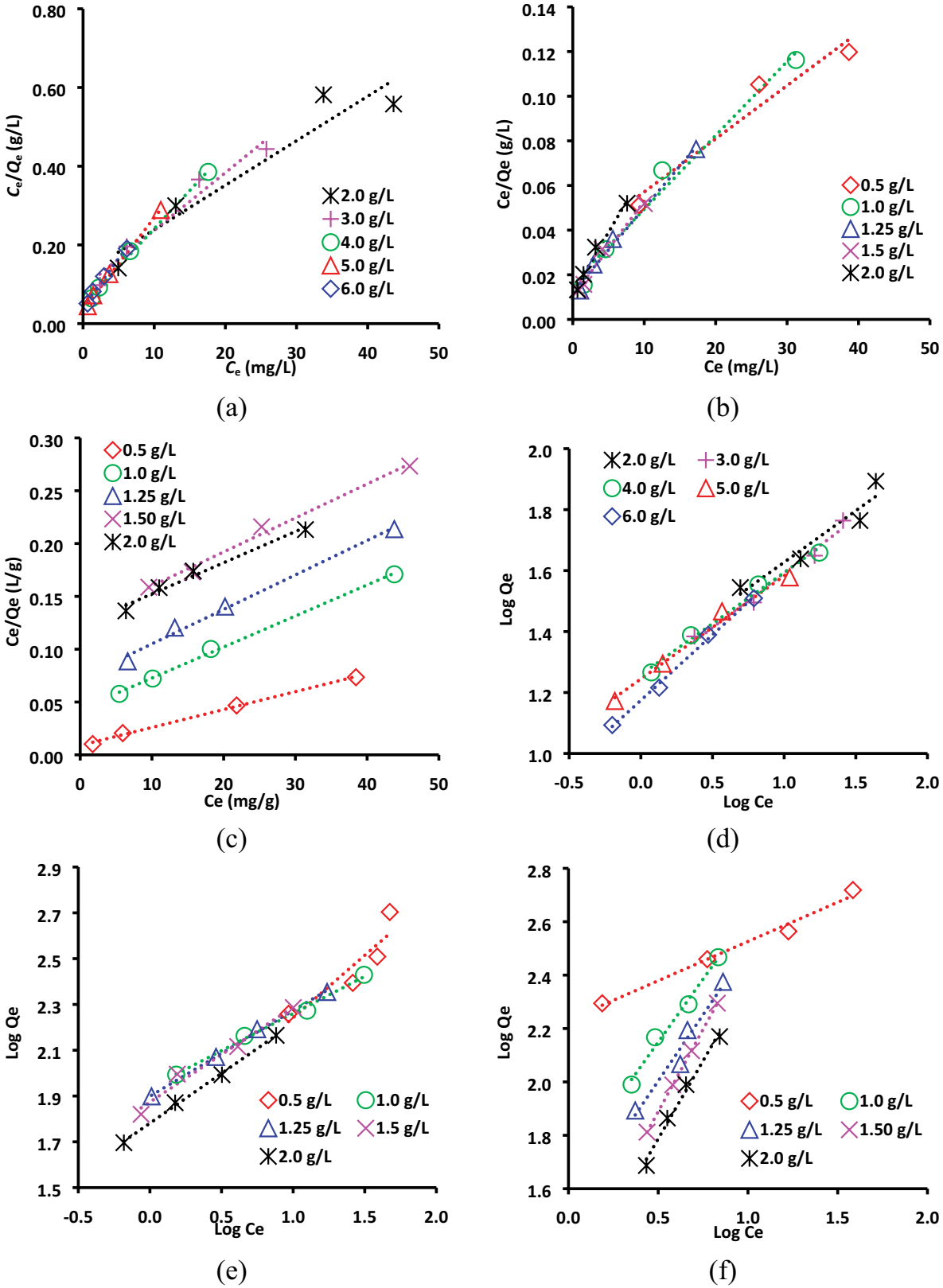

Fig. 12. Linearized Langmuir adsorption isotherm for AO7 dye of initial concentration (75–200 mg L^{-1}) on (a) Pea-B (2–6 g L^{-1}); AO7 dye of initial concentration (100–300 mg L^{-1}) on (b) Pea-BO-NH_2, (c) Pea-BO-TETA doses (0.5–2.0 g L^{-1}) at 25°C ± 2°C. Freundlich adsorption isotherm for AO7 dye of initial concentration (75–200 mg L^{-1}) on (d) Pea-B doses (2–6 g L^{-1}); Freundlich adsorption isotherm for AO7 dye of initial concentration (100–300 mg L^{-1}) on (e) Pea-BO-NH_2, and (f) Pea-BO-TETA doses (0.5–2.0 g L^{-1}) at 25°C ± 2°C.

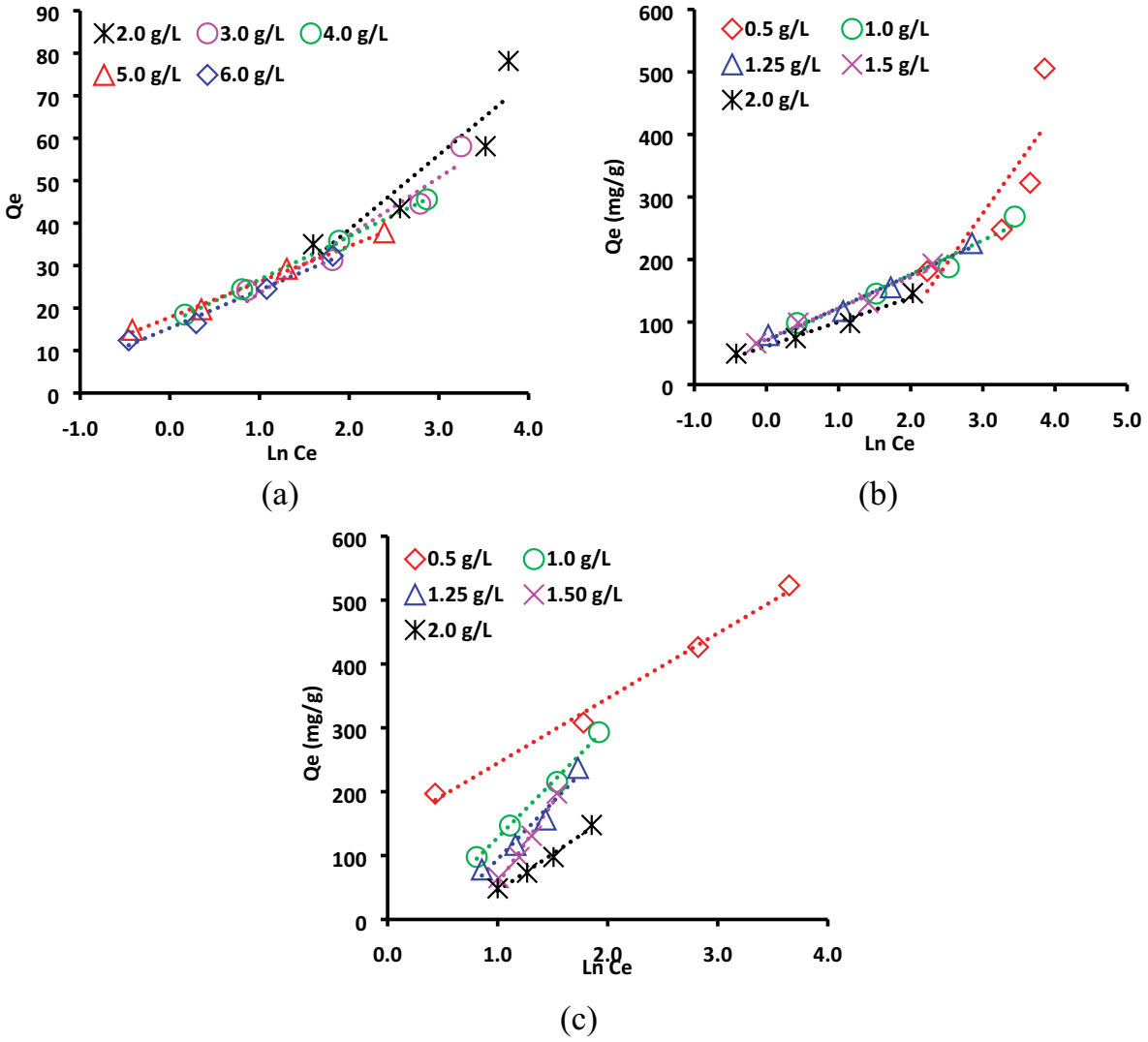

Fig. 13. Temkin adsorption isotherm for AO7 dye of initial concentration (75–200 mg L^{-1}) on (a) Pea-B (2–6 g L^{-1}); AO7 dye of initial concentration (100–300 mg L^{-1}) on (b) Pea-BO-NH_2, and (c) Pea-BO-TETA doses (0.5–2.0 g L^{-1}) at 25°C ± 2°C.

proved that the Temkin model fitted well with experimental data of the AO7 dye adsorption on three biochars. Tables 1–3 in supplement material reported the values of experimental and calculated q_e by using the Temkin model. In addition, from the results, we can deduce that the experimental and calculated q_e data are more applicable to increasing in adsorbent doses for the three biochars.

3.3.4. Error function studies for best-fit isotherm model

The best-fit isotherm model for the experimental data was studied by several different error functions. The applied error functions are the average percentage errors (APE) [55], Chi-square error (χ^2) [56], the root mean square errors (RMS) [55], the hybrid fractional error function (HYBRID) [57,58], the sum of the absolute errors (EABS) [55], and Marquardt's percent standard deviation (MPSD) [55] were applied to study the error distribution between the experimental and predicted data. The calculated isotherm parameters for Pea-B, Pea-BO-NH_2, and Pea-BO-TETA biochars using the six error functions are given in Table 3. From Table 3, it can be observed that the three isotherm models are comparable and applicable to the experimental equilibrium data. Also, from Table 3, it is clearly indicated that the error functions APE, χ^2, RMS, HYBRID, EABS, and MPSD do not take much effort in considering the theoretical limits of Freundlich isotherm, because it is the best-fit isotherm model for the experimental data.

3.4. Adsorption kinetic studies

3.4.1. Pseudo-first-order kinetic model

Adsorption reaction model, pseudo-first-order rate equation Lagergren [48] presented a first-order rate equation to describe the kinetic process of liquid-solid phase adsorption, which is believed to be the earliest model pertaining to the adsorption rate based on the adsorption capacity.

Table 3
Represent the best-fit isotherm model to the experimental equilibrium data by several different errors functions for Pea-B, Pea-BO-NH_2, and Pea-BO-TETA at 25°C ± 2°C

Pea-B	APE%	χ^2	HYBRID	MPSD	EABS	RMS
Linear-Langmuir	0.42	0.36	0.46	2.45	2.83	2.33
Freundlich	0.22	0.13	0.24	1.21	1.85	1.14
Temkin	0.29	0.22	0.32	1.73	2.21	1.64
Pea-BO-NH_2						
Linear-Langmuir	0.54	0.60	3.34	3.17	19.59	3.00
Freundlich	0.25	0.28	1.83	1.79	12.58	1.70
Temkin	0.44	0.48	2.98	2.57	18.39	2.44
Pea-BO-TETA						
Linear-Langmuir	0.68	0.75	6.35	4.38	23.74	4.15
Freundlich	0.19	0.21	0.42	1.21	2.71	1.15
Temkin	0.54	0.60	2.24	3.09	16.74	2.93

Straight-line plots of log ($q_e - q_t$) against t were used to determine the rate constant, k_1, and q_e, as shown in Fig. 14. Based on the values of R^2 obtained from the plots of pseudo-first-order rate equations (Tables 4–6), it is obvious that with increasing an initial concentration of the adsorbate, the correlation of experimental data to the pseudo-first-order model decrease. The theoretical values of q_e also not agree very well with the experimental ones. Both facts suggest that the adsorption of AO7 dye onto Pea-B, Pea-BO-NH_2 and Pea-BO-TETA biochars, did not follow pseudo-first-order kinetics.

3.4.2. Pseudo-second-order

The pseudo-second-order kinetic constant, k_2 (g mg^{-1} min^{-1}), and the amount of dye adsorbed at equilibrium q_e (mg g^{-1}) can be calculated from the intercept and slope of the plot between t/q_e vs. t. Fig. 14 shows pseudo-second-order kinetic plots for the sorption of AO7 dye over untreated and treated Pea-peels biochars. The calculated kinetic constant, k_2, the experimental, and theoretically predicted q_e as well as the corresponding R^2 values were shown in Tables 4–6. The relatively higher R^2 values for pseudo-second-order kinetics which are near equal to unity suggested that pseudo-second-order expression as a best fit kinetic model. In the present study, from Tables 4–6, the q_e values predicted using the pseudo-second-order plot are very close to the experimental q_e values, which confirms the applicability of the pseudo-second-order kinetic model. From Tables 4–6 it can be observed that, no definite relationship between the initial dye concentration and reaction rate constant, k_2.

3.4.3. Elovich model

The Elovich equation is a rate equation based on the adsorption capacity, generally expressed as reported in the theoretical background of this study. The data obtained from applying the Elovich equation to the experimental data of AO7 dye adsorption using Pea-B, Pea-BO-NH_2, and Pea-BO-TETA biochars are reported in Fig. 15 and Tables 7–9. The Elovich constants α and β were calculated from the intercept and slope of the straight line (Tables 7–9). It can observe that the correlation coefficients R^2 are disturbing without a definite role. The Elovich model provided a low degree of correlation with the experimental data for most of the sorption process. There was a discrepancy at the higher initial AO7 dye concentrations and different absorbent doses, which suggested that intraparticle diffusion may be involved in the sorption process. Results show that chemical adsorption processes were not the rate-limiting in the adsorption of AO7 dye onto the three biochars during agitated batch contact time experiments. The wavy value of R^2 obtained in the present study indicates that the adsorption of dye seems to involve physisorption as mention before.

3.4.4. Intraparticle diffusion model

Weber and Morris provided the intraparticle diffusion model equation as reported in the theoretical experimental section of this study. Webber and Morris thought that if the q_t and $t^{0.5}$ have a linear relation that passes the origin, the adsorption is controlled by intraparticle diffusion, however, if the line does not pass the origin, a larger C indicates that film diffusion greatly influences adsorption rate. Figs. 15d–f show the Weber–Morris adsorption line of AO7 dye adsorption onto the three biochars at different initial dye concentrations and different adsorbent doses. The values of C and K_{dif} are calculated from the intercept and slope of the plot of q_t against $t^{0.5}$, respectively, and represented in Tables 7–9. From Figs. 15d–f, we can deduce that the straight lines are not pass through the origin and the intercept C is quite large indicates that within time, the adsorption rate was faster and mainly does not controlled by the intraparticle diffusion, but the film diffusion was the dominant step that controlled the adsorption rate. This may be attributed to the surface area and pore volume which slightly reduced after treatment which shows intraparticle diffusion-based mechanism cannot account for dye adsorption enhancement. The values of C increased significantly for Pea-BO-NH_2 and Pea-BO-TETA than that for Pea-B biochars. It is speculated that it could be due to the electrostatic attraction between amino groups on the absorbents surface and the anionic AO7 dye.

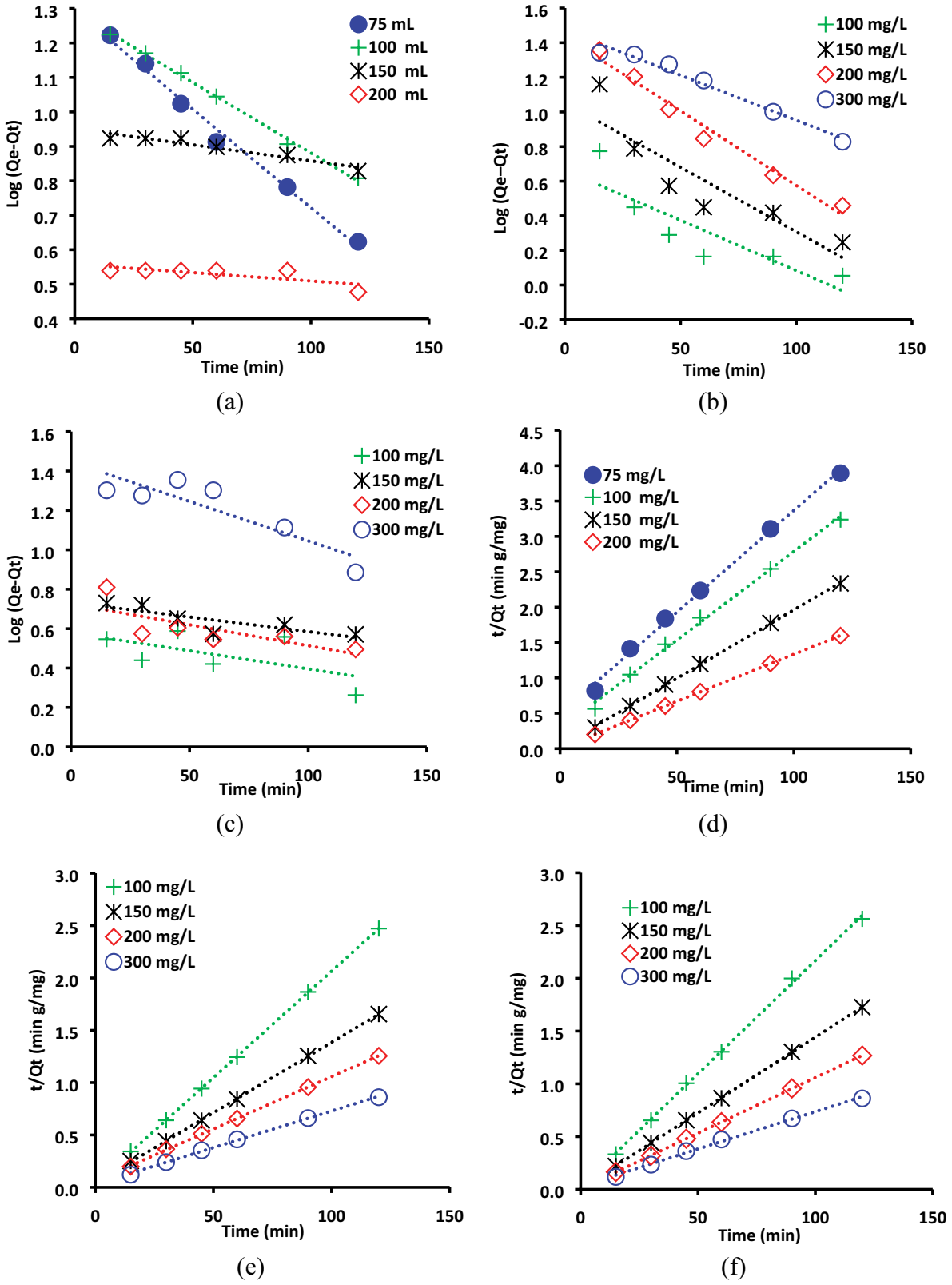

Fig. 14. Pseudo-first-order kinetic of adsorption of AO7 dye of initial concentration (75–200 mg L^{-1}) by (a) Pea-B; of initial concentration (100–300 mg L^{-1}) by (b) Pea-BO-NH_2, and (c) Pea-BO-TETA adsorbent dose (2.0 g L^{-1}) at 25°C ± 2°C. Pseudo-second-order kinetic of adsorption of AO7 dye of initial concentration (75–200 mg L^{-1}) by (d) Pea-B, (e) of initial concentration (100–300 mg L^{-1}) Pea-BO-NH_2, and (f) Pea-BO-TETA adsorbent dose (2.0 g L^{-1}) at 25°C ± 2°C.

Table 4
Pseudo-first-order and pseudo-second-order results of adsorption of AO7 dye of different initial concentration (75–200 mg L^{-1}) onto Pea-B of different adsorbent doses (2–6 g L^{-1} dye solution) at 25°C ± 2°C

Parameter			Pseudo-first-order			Pseudo-second-order			
Pea-B doses (g L^{-1})	AO7 dye (mg L^{-1})	$q_{e,exp.}$	$q_{e,cal.}$	$k_1 \times 10^3$	R^2	$q_{e,cal.}$	$k_2 \times 10^3$	h	R^2
2.0	75	35.03	19.66	13.127	0.991	34.84	1.67	2,030	0.997
	100	43.49	19.90	9.442	0.997	39.84	2.24	3,550	0.996
	150	58.11	8.94	2.073	0.627	51.55	15.81	42,017	1.000
	200	78.18	3.61	1.152	0.260	75.19	58.96	3.3E5	1.000
3.0	75	24.21	10.39	16.351	0.389	24.51	3.81	2,289	1.000
	100	31.29	15.54	13.357	0.623	30.96	2.35	2,256	0.997
	150	44.56	13.20	5.988	0.741	39.37	4.70	7,289	0.997
	200	58.08	8.56	0.921	0.636	50.76	29.63	7.6E4	1.000
4.0	75	18.45	6.86	18.654	0.941	18.90	6.06	2,166	1.000
	100	24.44	9.39	14.509	0.774	23.87	4.84	2,759	0.988
	150	35.85	12.18	4.376	0.977	29.50	6.28	5,464	0.997
	200	45.61	8.75	1.842	0.871	38.91	17.43	2.6E4	1.000
5.0	75	14.87	3.68	17.963	0.887	14.99	12.98	2,917	1.000
	100	19.72	6.38	18.885	0.935	20.08	6.94	2,797	1.000
	150	29.26	12.25	15.200	0.983	29.33	3.20	2,750	0.997
	200	37.82	9.43	5.988	0.904	34.13	6.34	7,380	0.997
6.0	75	12.40	1.87	14.509	0.786	12.27	29.47	4,437	1.000
	100	16.44	3.96	17.733	0.849	16.56	12.00	3,289	1.000
	150	24.51	9.26	18.194	0.939	25.06	4.37	2,748	0.998
	200	32.31	9.85	10.364	0.948	30.77	4.66	4,409	0.996

Table 5
Pseudo-first-order and pseudo-second-order results of adsorption of AO7 dye of different initial concentration (100–300 mg L^{-1}) onto Pea-BO-NH_2 of different adsorbent doses (0.5–2.0 g L^{-1} dye solution) at 25°C ± 2°C

Parameter			Pseudo-first-order			Pseudo-second-order			
Pea-BO-NH_2 doses (g L^{-1})	AO7 dye (mg L^{-1})	$q_{e,exp.}$	$q_{e,cal.}$	$k_1 \times 10^3$	R^2	$q_{e,cal.}$	$k_2 \times 10^3$	h	R^2
0.50	100	181.42	87.78	8.29	0.995	161.29	0.50	12,936	0.994
	150	247.84	51.71	1.84	0.929	208.33	3.11	135,135	1.000
	200	322.68	23.79	0.00	0.000	303.03	5.12	156,175	1.000
	300	505.47	8.58	0.00	0.000	500.00	–5E13	–1.2E19	1.000
1.00	100	98.47	25.21	16.12	0.884	98.04	1.92	18,484	1.000
	150	145.42	50.91	16.12	0.986	144.93	0.87	18,315	0.999
	200	187.47	45.97	6.45	0.931	172.41	1.26	37,593	0.998
	300	268.76	20.63	0.46	0.565	250.00	26.67	1.6E6	1.000
1.25	100	79.18	11.49	14.05	0.774	78.13	4.92	30,030	1.000
	150	117.68	36.08	19.11	0.986	119.05	1.29	18,248	1.000
	200	155.52	45.79	14.74	0.995	153.85	1.01	23,923	0.999
	300	226.19	29.19	1.84	0.872	204.08	5.11	2.1E5	1.000
1.50	100	66.09	8.33	13.59	0.790	65.36	6.99	29,850	1.000
	150	98.97	17.87	17.50	0.855	99.01	2.87	28,169	1.000
	200	130.60	34.95	19.11	0.975	131.58	1.40	24,271	1.000
	300	193.32	35.93	8.75	0.925	185.19	1.47	50,505	1.000
2.00	100	49.67	4.62	13.36	0.755	49.26	13.04	31,645	1.000
	150	74.25	11.33	17.27	0.805	74.07	4.61	25,316	1.000
	200	98.41	27.28	19.81	0.976	100.00	1.76	17,636	1.000
	300	146.20	29.62	11.98	0.975	142.86	1.67	34,013	0.999

Table 6
Pseudo-first-order and pseudo-second-order results of adsorption of AO7 dye of different initial concentration (100–300 mg L^{-1}) onto Pea-BO-TETA of different adsorbent doses (0.5–2.0 g L^{-1} dye solution) at 25°C ± 2°C

Parameter			Pseudo-first-order			Pseudo-second-order			
Pea-BO-TETA doses (g L^{-1})	AO7 dye (mg L^{-1})	$q_{e,exp.}$	$q_{e,cal.}$	$k_1 \times 10^3$	R^2	$q_{e,cal.}$	$k_2 \times 10^3$	h	R^2
0.50	100	196.92	77.62	5.99	0.976	193.93	0.83	2.24E+04	0.998
	150	288.14	71.53	0.46	0.709	282.22	15.58	7.69E+05	1.000
	200	366.40	50.59	0.46	0.706	362.58	19.22	2.00E+06	1.000
	300	523.12	8.73	0.00	0.000	526.32	4E+13	1.25E+19	1.000
1.00	100	97.75	10.75	12.44	0.458	96.15	4.89	4.52E+04	0.999
	150	146.96	33.05	15.43	0.773	147.06	1.40	3.02E+04	0.998
	200	195.33	45.84	11.05	0.950	198.68	1.13	4.02E+04	0.999
	300	293.17	37.53	0.01	0.000	296.41	76.05	5.00E+06	1.000
1.25	100	78.12	5.68	4.61	0.745	75.19	18.62	1.05E+05	1.000
	150	116.64	8.60	3.68	0.229	109.89	69.01	8.33E+05	1.000
	200	156.32	29.52	17.50	0.896	156.25	1.76	4.29E+04	1.000
	300	237.09	32.79	0.09	0.011	234.08	80.03	3.33E+06	1.000
1.50	100	64.84	3.06	–0.92	0.011	60.61	–19.17	–7.0E+04	0.999
	150	97.46	7.03	6.91	0.822	95.24	11.03	1.00E+05	1.000
	200	130.87	12.50	10.82	0.812	128.21	5.16	8.47E+04	1.000
	300	197.16	27.64	0.46	0.350	195.41	13.46	4.00E+05	1.000
2.00	100	48.64	3.80	4.15	0.351	46.51	20.64	4.46E+04	0.999
	150	73.22	5.41	3.45	0.700	69.93	25.25	1.23E+05	1.000
	200	97.74	5.32	4.84	0.571	95.24	21.20	1.92E+05	1.000
	300	147.81	27.93	9.21	0.784	145.85	1.72	3.41E+04	0.997

Table 7
Elovich and intraparticle diffusion models results of adsorption of AO7 dye of different initial concentration (75–200 mg L^{-1}) onto Pea-B of different adsorbent doses (2–6 g L^{-1} dye solution) at 25°C ± 2°C

Pea-B dose (g L^{-1})	AO7 initial conc. (mg L^{-1})	Elovich			Intraparticle diffusion		
		β	α	R^2	K_{dif}	C	R^2
2.0	75	0.16	7.26E+00	0.988	1.80	11.82	0.979
	100	0.19	5.16E+01	0.963	1.52	20.58	0.995
	150	1.34	3.17E+27	0.718	0.23	48.49	0.843
	200	6.87	3.90E+220	0.343	0.05	74.44	0.456
3.0	75	0.26	1.39E+01	0.983	1.07	11.74	0.923
	100	0.21	1.26E+01	0.992	1.42	13.12	0.986
	150	0.41	7.75E+04	0.843	0.76	29.52	0.939
	200	2.98	4.47E+62	0.540	0.11	49.20	0.681
4.0	75	0.36	1.65E+01	0.959	0.77	9.97	0.874
	100	0.31	3.05E+01	0.856	0.90	13.16	0.788
	150	0.54	5.81E+04	0.843	0.57	22.14	0.939
	200	1.62	5.12E+24	0.643	0.20	36.29	0.779
5.0	75	0.61	1.16E+02	0.914	0.45	9.97	0.806
	100	0.38	3.56E+01	0.946	0.73	11.72	0.853
	150	0.26	3.96E+01	0.931	1.12	15.36	0.954
	200	0.61	4.85E+06	0.720	0.52	27.15	0.848
6.0	75	1.12	6.62E+03	0.847	0.24	9.67	0.720
	100	0.54	1.11E+02	0.900	0.50	10.99	0.786
	150	0.30	3.31E+01	0.920	0.96	13.59	0.891
	200	0.43	4.87E+03	0.813	0.72	21.37	0.918

Table 8
Elovich and intraparticle diffusion models results of adsorption of AO7 dye of different initial concentration (100–300 mg L^{-1}) onto Pea-BO-NH_2 of different adsorbent doses (0.50–2.00 g L^{-1} dye solution) at 25°C ± 2°C

Pea-BO-NH_2 dose (g L^{-1})	AO7 initial conc. (mg L^{-1})	Elovich			Intraparticle diffusion		
		β	α	R^2	K_{dif}	C	R^2
0.50	100	0.047	1.54E+02	0.944	6.39	78.39	0.988
	150	0.267	1.65E+22	0.723	1.18	192.65	0.849
	200	2.5E+12	2.65E+22	–7E-15	0.00	298.89	0.000
	300	2.5E+12	4.65E+22	0.000	0.00	496.89	0.000
1.00	100	0.093	7.22E+02	0.932	2.95	65.02	0.832
	150	0.057	4.14E+02	0.992	4.99	86.00	0.960
	200	0.117	1.45E+07	0.763	2.67	135.75	0.883
	300	3.164	2.45E+09	0.343	0.11	247.83	0.456
1.25	100	0.185	8.56E+04	0.859	1.46	62.49	0.735
	150	0.072	4.77E+02	0.971	3.89	74.42	0.897
	200	0.070	3.69E+03	0.974	4.16	103.39	0.985
	300	0.472	4.40E+39	0.646	0.68	195.09	0.782
1.50	100	0.267	1.13E+06	0.879	1.01	54.25	0.760
	150	0.119	8.42E+03	0.882	2.29	74.12	0.764
	200	0.078	2.33E+03	0.980	3.63	89.96	0.921
	300	0.131	7.93E+08	0.763	2.40	153.30	0.883
2.00	100	0.458	1.12E+08	0.840	0.59	42.89	0.712
	150	0.174	1.98E+04	0.900	1.54	57.65	0.708
	200	0.100	1.38E+03	0.981	2.82	67.06	0.924
	300	0.129	3.45E+06	0.874	2.35	113.15	0.954

Table 9
Elovich and intraparticle diffusion models results of adsorption of AO7 dye of different initial concentration (100–300 mg L^{-1}) onto Pea-BO-TETA of different adsorbent doses (0.50–2.00 g L^{-1} dye solution) at 25°C ± 2°C

Pea-BO-NH_2 dose (g L^{-1})	AO7 initial conc. (mg L^{-1})	Elovich			Intraparticle diffusion		
		β	α	R^2	K_{dif}	C	R^2
0.50	100	0.06	1.81E+03	0.968	4.83	105.54	0.983
	150	0.63	4.90E+58	0.886	0.44	215.02	0.809
	200	1.02	1.13E+138	0.000	0.29	314.80	0.727
	300	1.25E+12	N/A	N/A	0.00	514.39	N/A
1.00	100	0.21	3.31E+07	0.648	1.31	81.79	0.609
	150	0.08	5.27E+03	0.812	3.77	103.14	0.772
	200	0.07	8.88E+04	0.927	3.95	140.69	0.949
	300	–227.27	0.00E+00	0.000	0.00	255.65	0.000
1.25	100	0.87	1.69E+26	0.846	0.32	71.33	0.786
	150	0.44	4.17E+19	0.561	0.56	105.30	0.408
	200	0.08	2.08E+04	0.919	3.49	117.65	0.817
	300	3.50	N/A	0.036	0.06	204.00	0.021
1.50	100	7.30	2.31E+192	0.010	–0.01	61.52	0.001
	150	0.54	1.54E+20	0.895	0.53	88.77	0.844
	200	0.21	1.09E+10	0.867	1.33	113.90	0.758
	300	1.92	6.17E+139	0.173	0.18	169.03	0.255
2.00	100	2.18	1.33E+41	0.203	0.15	44.52	0.245
	150	1.17	1.61E+33	0.809	0.24	66.97	0.773
	200	0.73	2.07E+28	0.735	0.36	90.98	0.617
	300	0.19	4.79E+09	0.513	1.74	117.10	0.651

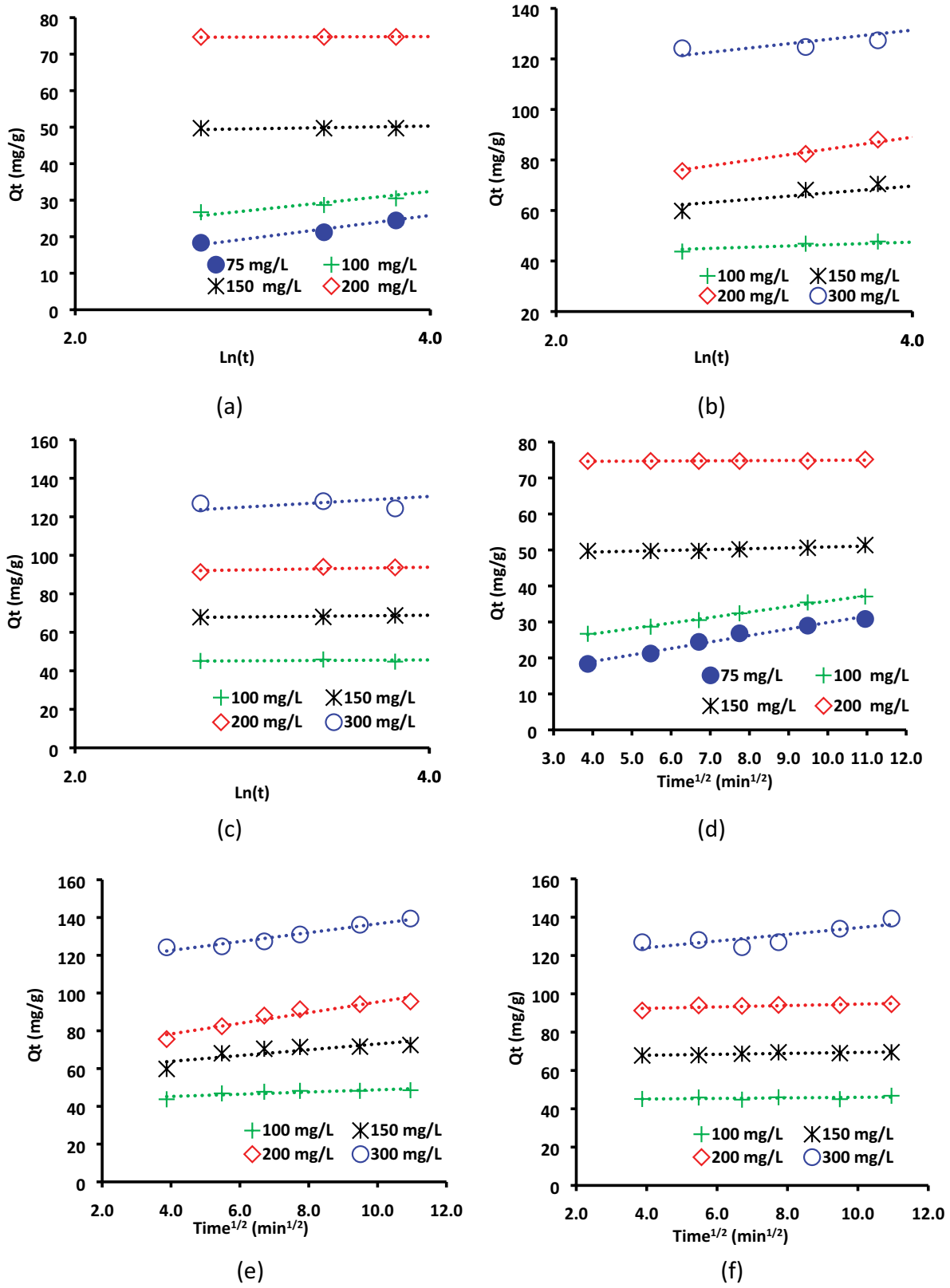

Fig. 15. Elovich kinetic of adsorption of AO7 dye of initial concentration (75–200 mg L^{-1}) by (a) Pea-B, of initial concentration (100–300 mg L^{-1}) by (b) Pea-BO-NH_2 and (c) Pea-BO-TETA adsorbent dose (2.0 g L^{-1}) at 25°C ± 2°C. Intraparticle diffusion of adsorption of AO7 dye of initial concentration (75–200 mg L^{-1}) by (d) Pea-B, of initial concentration (100–300 mg L^{-1}) by (e) Pea-BO-NH_2, and Pea-BO-TETA adsorbent dose (2.0 g L^{-1}) at 25°C ± 2°C.

4. Conclusion

In this research work, Pea-peels was chosen as the feedstock of biochar, based on which amino groups were successfully loaded by ozonation followed by reaction with ammonium hydroxide (NH_4OH or TETA). These biochars reveal remarkable removal efficiency and adsorption capacity for controlling water pollution by dissolved azo dyes Acid Orange 7 due to amino-containing functional groups on their surfaces. The excellent performance for the treatment of the AO7 dye was achieved via the batch adsorption method. Lower pH value favored AO7 dye removal by modified and unmodified Pea-peel biochars was evaluated to be pH 2. The other optimized process parameters for the maximum adsorption of AO7 dye were adsorbent dosage of 0.5 g L^{-1}, initial concentration of dye 300 mg L^{-1}, and contact time of 180 min. The equilibrium data for this study fitted very well to Freundlich isotherm. As for the order of the reaction, the rate of adsorption for the AO7 dye was found to comply with the pseudo-second-order kinetic model. These unique behaviors of modified and unmodified Pea-peel biochars may be considered as feasible waste resource utilization that converts the agricultural solid waste into stable, cheap, and multifunctional bio-resource.

References

[1] A. El Nemr, Impact, Monitoring and Management of Environmental Pollution, Nova Science Publishers, Inc. Hauppauge, New York, [ISBN-10: 1608764877, ISBN-13: 9781608764877], 2011, p. 638.

[2] A. El Nemr, Pollution Status, Environmental Protection, and Renewable Energy production in Marine Systems, Nova Science Publishers, Inc. Hauppauge, New York, 2016.

[3] K. Itoh, Y. Kitade, C. Yatote, A pathway for biodegradation of an anthraquinone dye, C.I. disperse red 15, by a yeast strain *Pichia anomala*, Bull. Environ. Contam. Toxicol., 56 (1996) 413–418.

[4] P.C. Vandevivere, R. Bianchi, W. Verstraete, Biodegradation and decolorization of reactive dye red ME4BL by *Bacillus subtilis*, J. Chem. Technol. Biotechnol., 72 (1998) 289–302.

[5] B.D. Tony, D. Goyal, S. Khanna, Decolorization of textile azo dyes by aerobic bacterial consortium, Int. Biodeterior. Biodegrad., 63 (2009) 462–469.

[6] R.D. Ambashta, M. Sillanpää, Water purification using magnetic assistance: a review, J. Hazard. Mater., 180 (2010) 38–49.

[7] A.B. Santos, F.J. Cervantes, J.B. Lier, Review paper on current technologies for decolorization of textile wastewaters: perspectives for anaerobic biotechnology, Bioresour. Technol., 98 (2007) 2369–2385.

[8] A. El Nemr, Textiles: Types, Uses and Production Methods, Nova Science Publishers, Inc. Hauppauge, New York, 2012, p. 621.

[9] K. Qureshi, M.Z. Ahmad, I.A. Bhatti, M. Iqbal, A. Khan, Cytotoxicity reduction of wastewater treated by advanced oxidation process, Chem. Int., 1 (2015) 53–59.

[10] C. Rafols, D. Barcelo, Determination of mono- and disulphonated azo dyes by liquid chromatography-atmospheric pressure ionization mass spectrometry, J. Chromatogr. A, 279 (1997) 177–192.

[11] G. Crini, Non-conventional low-cost adsorbents for dye removal: a review, Bioresour. Technol., 97 (2006) 1061–1085.

[12] M. Rafatullah, O. Sulaiman, R. Hashim, A. Ahmad, Adsorption of methylene blue on low-cost adsorbents: a review, J. Hazard. Mater., 177 (2010) 70–80.

[13] Y.J. Yao, B. He, F.F. Xu, X.F. Chen, Equilibrium and kinetic studies of methyl orange adsorption on multiwalled carbon nanotubes, Chem. Eng. J., 170 (2011) 82–89.

[14] A. El Nemr, Non-Conventional Textile Waste Water Treatment, Nova Science Publishers, Inc. Hauppauge, New York, 2012, p. 267.

[15] M.R. Awual, G.E. Eldesoky, T. Yaita, Schiff based ligand containing nano-composite adsorbent for optical copper(II) ions removal from aqueous solutions, Chem. Eng. J., 279 (2015) 639–647.

[16] S. Liakou, M. Kornaros, G. Lyberatos, Ozonation of azo-dyes, Water Sci. Technol., 35 (1997) 279–286.

[17] A.A. Moneer, A. El Nemr, Electro-Coagulation for Textile Dyes Removal, A. El Nemr, Ed., Non-Conventional Textile Waste Water Treatment, Nova Science Publishers, Inc. Hauppauge, New York, 2012, pp. 161–204.

[18] A. El Nemr, A. Khaled, O. Abdelwahab, A. El-Sikaily, Treatment of artificial textile dye effluent containing direct yellow 12 by orange peel carbon, Desalination, 238 (2009) 210–232.

[19] A. El Nemr, A. El-Sikaily, A. Khaled, Modeling of adsorption isotherms of methylene blue onto rice husk activated carbon, Egypt. J. Aquat. Res., 36 (2010) 403–425.

[20] A. El Nemr, M.M. El Sadaawy, A. Khaled, A. El Sikaily, Adsorption of the anionic dye direct red 23 onto new activated carbons developed from *Cynara cardunculus*: kinetics, equilibrium and thermodynamics, Blue Biotechnol. J., 3 (2014) 121–142.

[21] M.A. Hassaan, A. El Nemr, F.F. Madkou, Testing the advanced oxidation processes on the degradation of direct blue 86 dye in wastewater, Egypt. J. Aquat. Res., 43 (2017) 11–19.

[22] A. El Nemr, M.A. Hassaan, F.F. Madkour, Advanced oxidation process (AOP) for detoxification of acid red 17 dye solution and degradation mechanism, Environ. Process., 5 (2018) 95–113.

[23] E.T. Helmy, A. El Nemr, M. Mousa, E. Arafa, S. Eldafrawy, Photocatalytic degradation of organic dyes pollutants in the industrial textile wastewater by using synthesized TiO_2, C-doped TiO_2, S-doped TiO_2 and C,S co-doped TiO_2 nanoparticles, J. Water Environ. Nanotechnol., 3 (2018) 116–127.

[24] V.K. Garg, R. Kumar, R. Gupta, Removal of malachite green dye from aqueous solution by adsorption using agroindustry waste: a case study of *Prosopis cineraria*, Dyes Pigm., 62 (2004) 1–10.

[25] B. Chen, Z. Chen, S. Lv, A novel magnetic biochar efficiently sorbs organic pollutants and phosphate, Bioresour. Technol., 102 (2011) 716–723.

[26] Y. Liu, Characterization of bio-char from pyrolysis of wheat straw and its evaluation on methylene blue adsorption, Desal. Water Treat., 46 (2012) 115–123.

[27] S.-Y. Wang, Combined performance of biochar sorption and magnetic separation processes for treatment of chromium contained electroplating wastewater, Bioresour. Technol., 174 (2014) 67–73.

[28] D.H.K. Reddy, S.-M. Lee, Magnetic biochar composite: facile synthesis, characterization, and application for heavy metal removal, Colloids Surf., A, 454 (2014) 96–103.

[29] P. Devi, A.K. Saroha, Synthesis of the magnetic biochar composites for use as an adsorbent for the removal of pentachlorophenol from the effluent, Bioresour. Technol., 169 (2014) 525–531.

[30] Mu. Naushad, Z.A. Alothman, Md. Rabiul Awual, S.M. Alfadul, T. Ahamad, Adsorption of rose Bengal dye from aqueous solution by amberlite Ira-938 resin: kinetics, isotherms, and thermodynamic studies, Desal. Water Treat., 57 (2016) 13527–13533.

[31] Mu. Naushad, A.A. Alqadami, Z.A. AlOthman, I.H. Alsohaimi, M.S. Algamdi, A.M. Aldawsari, Adsorption kinetics, isotherm and reusability studies for the removal of cationic dye from aqueous medium using arginine modified activated carbon, J. Mol. Liq., 293 (2019) 111442.

[32] N.S. Shah, J.A. Khan, M. Sayed, Z. Ul Haq Khan, H.M. Khan, Synergistic effects of H_2O_2 and $S_2O_8^{2-}$ in the gamma radiation induced degradation of congo-red dye: kinetics and toxicities evaluation, Sep. Purif. Technol., 233 (2020) 115966.

[33] L. Han, S. Xue, S. Zhao, J. Yan, L. Qian, M. Chen, Biochar supported nanoscale iron particles for the efficient removal of methyl orange dye in aqueous solutions, PLoS One, 10 (2015) 0132067.

[34] S.J. Gregg, K.S.W. Sing, Adsorption Surface Area and Porosity, 2nd ed., Academic Press Inc., London, 1982.
[35] F. Rouquerol, J. Rouquerol, K.S.W. Sing, Adsorption by Powders and Porous Solids, Academic Press Inc., London, 1999.
[36] E.P. Barrett, L.G. Joyner, P.P. Halenda, The determination of pore volume and area distributions in porous substances, I. Computations from nitrogen isotherms, J. Am. Chem. Soc., 73 (1951) 373–380.
[37] I. Langmuir, The constitution and fundamental properties of solids and liquids, J. Am. Chem. Soc., 38 (1916) 2221–2295.
[38] M. Doğan, M. Alkan, Y. Onganer, Adsorption of methylene blue from aqueous solution onto perlite, Water Air Soil Pollut., 120 (2000) 229–249.
[39] H.M.F. Freundlich, Über die adsorption inlösungen, Z. Phys. Chem., (Leipzig), 57A (1906) 385–470.
[40] G.D. Halsey, Physical adsorption in non-uniform surfaces, J. Chem. Phys., 16 (1948) 931–945.
[41] M.J. Temkin, V. Pyzhev, Kinetics of ammonia synthesis on promoted iron catalysts, Acta Physiochim., URSS, 12 (1940) 217–222.
[42] D. Kavitha, C. Namasivayam, Experimental and kinetic studies on methylene blue adsorption by coirpith carbon, Bioresour. Technol., 98 (2007) 14–21.
[43] C. Aharoni, M. Ungarish, Kinetics of activated chemisorptions, Part 2. Theoretical models, J. Chem. Soc., Faraday Trans., 73 (1977) 456–464.
[44] C. Aharoni, D.L. Sparks, Kinetics of Soil Chemical Reactions – A Theoretical Treatment, D.L. Sparks, D.L. Suarez, Eds., Rate of Soil Chemical Processes, Soil Science Society of America, Madison, WI, 1991, pp. 1–18.
[45] X.S. Wang, Y. Qin, Equilibrium sorption isotherms for of Cu^{2+} on rice bran, Process Biochem., 40 (2005) 677–680.
[46] C.I. Pearce, J.R. Lioyd, J.T. Guthrie, The removal of color from textile wastewater using whole bacterial cells: a review, Dyes Pigm., 58 (2003) 179–196.
[47] G. Akkaya, A. Ozer, Biosorption of acid red 274(AR 274) on *Dicranella varia*: determination of equilibrium and kinetic model parameters, Process Biochem., 40 (2005) 3559–3568.
[48] S. Lagergren, Zurtheorie der sogenannten adsorption gelosterstoffe, Kungliga Svenska Vetenskapsakademiens, Handlingar, 24 (1898) 1–39.
[49] Y.S. Ho, G. McKay, D.A.J. Wase, C.F. Foster, Study of the sorption of divalent metal ions onto peat, Adsorpt. Sci. Technol., 18 (2000) 639–650.
[50] J. Zeldowitsch, Über den mechanismus derkatalytischen oxidation von CO and MnO_2, Acta Physicochim., URSS, 1 (1934) 364–449.
[51] S.H. Chien, W.R. Clayton, Application of Elovich equation to the kinetics of phosphate release and sorption on soils, Soil Sci. Soc. Am. J., 44 (1980) 265–268.
[52] D.L. Sparks, Kinetics of Reaction in Pure and Mixed Systems, In: Soil Physical Chemistry, CRC Press, Boca Raton, 1986.
[53] W.J. Weber, J.C. Morris, Kinetics of adsorption on carbon from solution, J. Sanit. Eng. Div. Am. Soc. Civil Eng., 89 (1963) 31–60.
[54] K. Srinivasan, N. Balasubramanian, T.V. Ramakrishan, Studies on chromium removal by rice husk carbon, Indian J. Environ. Health, 30 (1988) 376–387.
[55] J.C.Y. Ng, W.H. Cheung, G. McKay, Equilibrium studies of the sorption of Cu(II) ions onto chitosan, J. Colloid Interface Sci., 255 (2002) 64–74.
[56] Y.S. Ho, W.T. Chiu, C.C. Wang, Regression analysis for the sorption isotherms of basic dyes on sugarcane dust, Bioresour. Technol., 96 (2005) 1285–1291.
[57] J.F. Porter, G. McKay, K.H. Choy, The prediction of sorption from a binary mixture of acidic des using single- and mixed-isotherm variants of the ideal adsorbed solute theory, Chem. Eng. Sci., 54 (1999) 5863–5885.
[58] S.J. Allen, Q. Gan, R. Matthews, P.A. Johnson, Comparison of optimized isotherm models for basic dye adsorption by kudzu, Bioresour. Technol., 88 (2003) 143–152.

Supplementary information

Table S1
Relation between q_e (mg/g) of AO7 dye at different initial concentrations (75, 100, 150, and 200 mg/L) obtained by batch experimental and q_e (mg/g) calculated using data obtained from different isotherm models using different doses of Pea-B (2–6 g/L) at 25°C ± 2°C

Isotherm			Langmuir	Freundlich	Temkin
Pea-B dose (g/L)	AO7 initial conc. (mg/L)	$q_{e,\text{exp.}}$ (mg/g)	$q_{e,\text{cal.}}$ (mg/g)	$q_{e,\text{cal.}}$ (mg/g)	$q_{e,\text{cal.}}$ (mg/g)
2.0	75	35.03	27.28	33.42	31.72
	100	48.07	47.78	46.36	48.91
	150	58.11	66.61	63.99	65.84
	200	78.18	70.55	69.76	70.38
3.0	75	24.21	18.89	23.32	21.61
	100	31.29	34.00	32.81	34.56
	150	44.56	49.59	46.62	47.87
	200	58.08	55.17	54.93	54.09
4.0	75	18.45	16.78	19.20	18.28
	100	24.44	24.58	23.76	24.73
	150	35.85	37.58	34.13	35.71
	200	45.61	45.23	47.37	45.63
5.0	75	14.87	12.98	15.24	14.31
	100	19.72	20.73	19.78	20.76
	150	29.26	30.32	27.30	28.74
	200	37.82	37.55	39.43	37.85
6.0	75	12.40	10.74	12.26	11.25
	100	16.44	17.62	16.95	17.95
	150	24.51	25.56	23.78	24.95
	200	32.31	31.80	32.64	31.51

Table S2
Relation between q_e (mg/g) of AO7 dye at different initial concentrations (100, 150, 200, and 300 mg/L) obtained by batch experimental and q_e (mg/g) calculated using data obtained from different isotherm models using different doses of Pea-BO-NH_2 (0.5–2.0 g/L) at 25°C ± 2°C

Isotherm			Langmuir	Freundlich	Temkin
Pea-BO-NH_2 dose (g/L)	AO7 initial conc. (mg/L)	$q_{e,exp.}$ (mg/g)	$q_{e,cal.}$ (mg/g)	$q_{e,cal.}$ (mg/g)	$q_{e,cal.}$ (mg/g)
0.50	100	181.42	142.61	167.79	149.39
	150	247.84	299.88	294.38	316.11
	200	322.68	374.17	364.76	379.68
	300	505.47	412.77	406.95	412.14
1.00	100	98.47	71.54	98.95	90.18
	150	145.42	145.80	141.31	150.11
	200	187.47	217.34	195.85	204.99
	300	268.76	261.66	263.40	254.83
1.25	100	79.18	63.35	80.00	71.70
	150	117.68	124.26	117.94	126.15
	200	155.52	166.83	151.01	160.83
	300	226.19	221.61	230.05	219.88
1.50	100	66.09	61.36	70.50	65.34
	150	98.97	91.23	89.73	94.23
	200	130.60	147.98	134.27	142.51
	300	193.32	190.57	194.43	186.87
2.00	100	49.67	42.60	50.36	45.01
	150	74.25	75.02	72.08	77.05
	200	98.41	109.46	100.02	106.31
	300	146.20	143.60	146.10	140.16

Table S3
Relation between q_e (mg/g) of AO7 dye at different initial concentrations (100, 150, 200, and 300 mg/L) obtained by batch experimental and q_e (mg/g) calculated using data obtained from different isotherm models using different doses of Pea-BO-TETA (0.5–2.0 g/L) at 25°C ± 2°C

Isotherm			Langmuir	Freundlich	Temkin
Pea-BO-TETA dose (g/L)	AO7 initial conc. (mg/L)	$q_{e,\text{exp.}}$ (mg/g)	$q_{e,\text{cal.}}$ (mg/g)	$q_{e,\text{cal.}}$ (mg/g)	$q_{e,\text{cal.}}$ (mg/g)
0.50	100	196.92	185.57	193.77	186.27
	150	288.14	310.75	287.92	286.01
	200	366.40	373.30	371.04	376.30
	300	523.12	517.03	518.73	526.00
1.00	100	97.75	92.30	102.10	92.80
	150	146.96	139.16	135.77	143.72
	200	195.33	189.49	203.51	201.03
	300	293.17	277.15	291.52	289.23
1.25	100	78.12	70.19	75.14	80.62
	150	116.64	113.75	133.43	114.85
	200	156.32	145.22	146.30	163.75
	300	237.09	231.88	230.17	234.79
1.50	100	64.84	60.43	64.84	64.49
	150	97.46	87.93	97.35	102.51
	200	130.87	121.22	131.01	131.02
	300	197.16	187.21	197.04	192.38
2.00	100	48.64	44.94	51.32	45.71
	150	73.22	70.61	70.18	76.86
	200	97.74	92.69	95.86	101.80
	300	147.81	144.71	151.76	147.78